Research Square

Preprints are preliminary reports that have not undergone peer review.
They should not be considered conclusive, used to inform clinical practice,
or referenced by the media as validated information.

Prognostic value of TyG-ABSI for all-cause and cardiovascular mortality across metabolic syndrome-related obesity phenotypes: a nationwide cohort study

Qianqian Xiang[1]
Bishan Hospital of Chongqing Medical University
Mengru Xiang[1]
Bishan Hospital of Chongqing Medical University
Min Lu[2]
islandnoone@foxmail.com

Bishan Hospital of Chongqing Medical University

Research Article

Keywords: Triglyceride-glucose index, A Body Shape Index, Metabolic syndrome, Obesity phenotypes, Insulin resistance, Cardiovascular mortality, Risk stratification

Posted Date: November 16th, 2026

DOI: https://doi.org/10.21203/rs.3.rs-11318202/v1

License: This work is licensed under a Creative Commons Attribution 4.0 International License.
Read Full License

Additional Declarations: No competing interests reported.

Prognostic value of TyG-ABSI for all-cause and cardiovascular mortality across metabolic syndrome-related obesity phenotypes: a nationwide cohort study

Qianqian Xiang[1], Mengru Xiang[1], Min Lu[2]*

[1]Department of General Medicine, Bishan Hospital of Chongqing Medical University, Chongqing, 402760 China

[2]Department of Ultrasound, Bishan Hospital of Chongqing Medical University, Chongqing, 402760 China

*Corresponding author(s). E-mail(s): islandnoone@foxmail.com; Contributing authors: 13883155666@163.com; 1933572155@qq.com;

Abstract

Background: Metabolic syndrome (MetS) and its related phenotypes are major drivers of cardiovascular mortality. The triglyceride-glucose (TyG) index and A Body Shape Index (ABSI) reflect insulin resistance and visceral adiposity, respectively. Their composite metric, TyG-ABSI, integrates these dimensions, but its predictive value for mortality across MetS-related metabolic health–obesity phenotypes remains unclear.

Methods: This study included 20,430 adults aged ≥ 20 years from the National Health and Nutrition Examination Survey (NHANES) 1999–2018. Participants were classified into four MetS-related phenotypes—metabolically healthy non-obesity (MHNO), metabolically healthy obesity (MHO), metabolically unhealthy non-obesity (MUNO), and metabolically unhealthy obesity (MUO)—according to body mass index and the American Heart Association/National Heart, Lung, and Blood Institute (AHA/NHLBI) criteria. Weighted Cox regression, restricted cubic splines, Fine–Gray competing risk models, and time-dependent receiver operating characteristic (ROC) analysis were em-

ployed. Stratified analyses by estimated pulse wave velocity (ePWV) were performed to assess effect modification by an ePWV-related vascular aging process, supplemented by an exploratory association decomposition analysis. A preliminary cross-population comparison was also conducted in the CHARLS cohort (n = 7,239).

Results: During a median follow-up of 115 months, 2,524 all-cause and 774 cardiovascular deaths occurred. Each 1-SD increase in TyG-ABSI was associated with higher all-cause (HR 1.19, 95% CI 1.12–1.25) and cardiovascular mortality (HR 1.27, 95% CI 1.14–1.41). Associations were linear in MUNO and MUO, nonlinear in MHNO, and not statistically significant in MHO, though limited events warrant caution. TyG-ABSI achieved the highest 15-year AUCs in the overall population but showed no incremental value in MHO. Exploratory association decomposition analyses did not support causal inference, and sensitivity analyses were generally consistent. In a preliminary CHARLS comparison, the primary findings were not replicated, suggesting potential population-specific effects.

Conclusions: Across MetS-related obesity phenotypes, TyG-ABSI showed phenotype-dependent prognostic performance, with the most consistent independent value in MUNO. In MUO, its association was largely explained by conventional MetS components, whereas in MHO no significant association was detected. These findings suggest TyG-ABSI may aid risk stratification in MUNO, but its value in MUO is largely captured by conventional MetS components.

Keywords: Triglyceride-glucose index; A Body Shape Index; Metabolic syndrome; Obesity phenotypes; Insulin resistance; Cardiovascular mortality; Risk stratification.

Research Insights

What is already known about this topic?	- TyG index is a reliable surrogate marker of insulin resistance associated with cardiovascular risk. - ABSI reflects visceral fat distribution independent of body weight. - Whether TyG-ABSI adds prognostic value across MetS-related metabolic health–obesity phenotypes remains unclear.
What is the key research question?	Does TyG-ABSI predict mortality differently across MetS-related metabolic–obesity phenotypes in U.S. adults?
What is new?	- Each 1-SD increase in TyG-ABSI raised all-cause and cardiovascular mortality by 19% and 27%. - Associations were linear in unhealthy phenotypes, nonlinear in MHNO, and not statistically significant in MHO. - TyG-ABSI retained independent prognostic value in MUNO but was largely explained by conventional MetS components in MUO.

How will this study impact clinical practice?	TyG-ABSI may aid risk stratification in MUNO, whereas its value in MUO is largely captured by conventional MetS components. Evidence in MHO remains limited.

1 Introduction

Cardiovascular disease (CVD) remains the leading cause of death and disability worldwide, posing a major public health challenge [1, 2]. The interaction between metabolic syndrome (MetS) and obesity is a key driver of cardiovascular disease and premature mortality [3]. Traditionally, obesity is defined by body mass index (BMI ≥ 30 kg/m²); however, some obese individuals exhibit normal metabolic profiles—termed metabolically healthy obesity (MHO) [4]—while others with normal BMI have metabolic disorders, termed metabolically unhealthy non-obesity (MUNO) [4]. This overlap highlights the limitations of BMI-based risk stratification and underscores the need for biomarkers that integrate metabolic function and body composition. These four phenotypes—MHNO, MHO, MUNO, and MUO—represent distinct MetS-related metabolic health–obesity phenotypes.

Insulin resistance is a core pathophysiological link connecting obesity, metabolic disorders, and cardiovascular events [5-7]. The triglyceride-glucose (TyG) index is a simple surrogate for insulin resistance and is associated with type 2 diabetes, atherosclerotic cardiovascular disease, and all-cause mortality [8-10]. However, TyG only reflects metabolic aspects and does not account for fat distribution. The A Body Shape Index (ABSI), derived from waist circumference, height, and BMI, independently quantifies visceral fat distribution and is associated with cardiovascular mortality and acute coronary syndrome [10, 11].

The combination of TyG and ABSI forms the TyG-ABSI, which theoretically captures both metabolic dysfunction and central obesity. Previous studies have shown that TyG-ABSI predicts cardiovascular mortality better than traditional indices such as TyG-BMI [12], and its superiority has been confirmed in populations with MASLD [13], hypertension [14], and MetS [15]. However, these studies either focused on MetS populations or analyzed the overall population without stratifying by metabolic health–obesity phenotypes. This leaves a critical clinical question unanswered: does the predictive value of TyG-ABSI differ across phenotypes—particularly, does it retain significance in MHO, where metabolic health may offset obesity-related risk? Clarifying this is essential for defining the target population for TyG-ABSI and avoiding unnecessary testing in low-risk individuals.

Unlike previous studies that focused on MetS populations or overall populations, this study was designed to evaluate whether the prognostic value of TyG-ABSI is phenotype-dependent across all four metabolic health–obesity phenotypes. In particular, we aimed to determine whether TyG-ABSI retains independent predictive value in MUNO, whether its association is largely explained by conventional MetS components in MUO, and whether it provides useful risk stratification in MHO.

Therefore, this study aimed to evaluate whether the prognostic value of TyG-ABSI is phenotype-dependent across four MetS-related metabolic health–obesity phenotypes, using data from NHANES 1999–2018. Specifically, we aimed to: (1) assess the association between TyG-ABSI and all-cause and cardiovascular mortality across phenotypes; (2) characterize dose–response relationships using restricted cubic splines; (3) compare predictive performance with other TyG-derived indices and evaluate incremental value; and (4) explore effect modification by ePWV and perform a preliminary cross-population comparison in CHARLS.

2 Methods

2.1 Study design and population

This study was reported following the STROBE statement for cohort studies (see **Supplementary Material 5**).The National Health and Nutrition Examination Survey (NHANES) is a nationally representative survey employing a complex, multistage probability sampling design, with data collected through in-person interviews, physical examinations, and laboratory tests. This study pooled ten survey cycles from 1999 to 2018, applying 20-year follow-up weights to ensure representativeness. Mortality data were ascertained through NHANES-linked National Death Index records with follow-up through December 31, 2019.

The China Health and Retirement Longitudinal Study (CHARLS) is a nationally representative cohort of Chinese residents aged ≥ 45 years and their spouses, using a multistage probability-proportional-to-size sampling design covering both urban and rural areas. This study used baseline data from the first wave (May 2011–March 2012), which included 17,708 individuals from 10,257 households across 450 villages/communities in 150 counties of 28 provinces. Participants with complete key variables were included; those with missing key variables were excluded. Mortality was confirmed through follow-up interviews (2013, 2015, 2018, and 2020) via proxy interviews, medical records, and local death registries, with follow-up through 2020. CHARLS only provides all-cause mortality data without cause-specific information. The CHARLS study was approved by the Biomedical Ethics Review Committee of Peking University (approval No. IRB00001052-11015), and written informed consent was obtained from all participants prior to enrollment.

2.2 Study population

To construct the analytic cohort from NHANES (1999–2018), we applied the exclusion criteria

shown in **Figure 1**. In brief, we excluded individuals with: age < 18 or > 85 years (n = 42,122), pregnancy (n = 809), fasting time < 8 hours (n = 29,185), BMI < 18.5 kg/m² (n = 1,067), missing key anthropometric or laboratory data (n = 6,574), missing liver/renal function data (n = 35), missing or extreme blood pressure values (n = 585 and 372, respectively), missing mortality follow-up (n = 26), or follow-up < 1 year (n = 121). This yielded 20,430 eligible participants for the final analysis (**Figure 1**).

Based on the inclusion and exclusion criteria detailed in **Figure 2**, participants from the CHARLS cohort were excluded if they met any of the following conditions: (1) age < 45 years or > 85 years (n = 792); (2) missing data for weight, height, or waist circumference (n = 3,848); (3) missing data for triglycerides or blood glucose (n = 3,655); (4) BMI < 18.5 kg/m² (n = 638); or (5) follow-up duration < 1 year (n = 1,536). This yielded a final analytic sample of 7,239 participants (**Figure 2**).

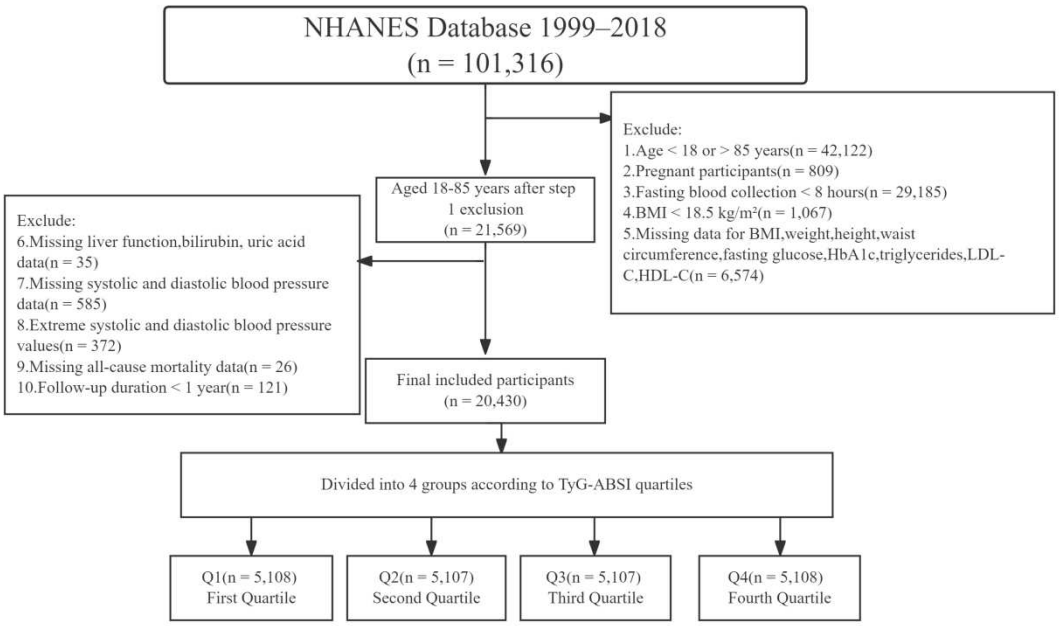


Figure 1. Flowchart of participant selection in the NHANES (1999–2018) cohort. NHANES: National Health and Nutrition Examination Survey; TyG: triglyceride-glucose index; ABSI: A Body Shape Index; BMI: body mass index; Q: quartile.

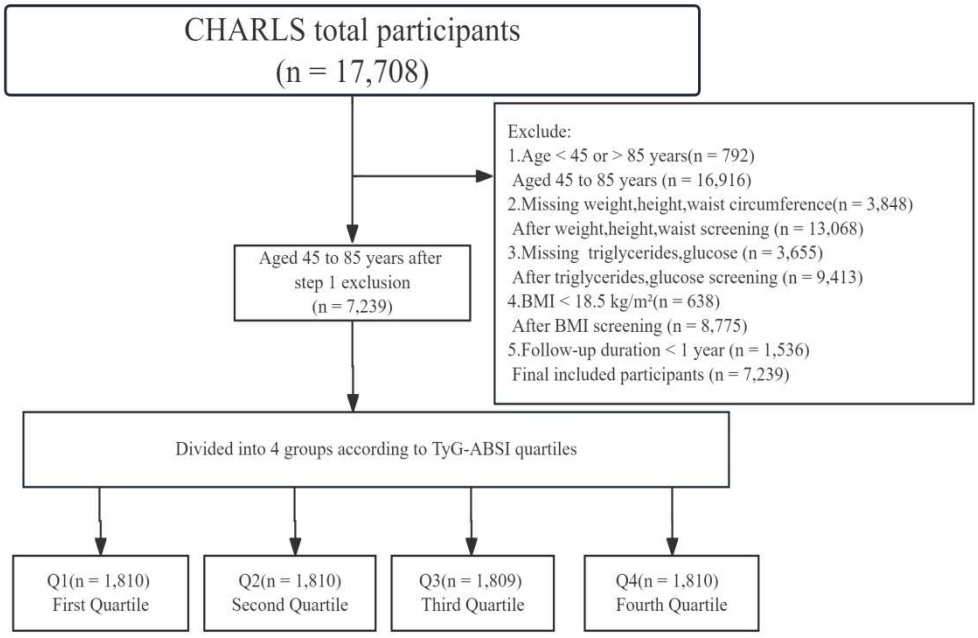


Figure 2. Flowchart of participant selection in the CHARLS cohort. CHARLS: China Health and Retirement Longitudinal Study; TyG: triglyceride-glucose index; ABSI: A Body Shape Index; BMI: body mass index; Q: quartile.

2.3 Metabolic health and obesity phenotypes

MetS-related metabolic health–obesity phenotypes were defined based on obesity status and metabolic health. Participants enrolled in the NHANES database were classified into the obese group (BMI ≥ 30 kg/m²) and the non-obesity group (BMI < 30 kg/m²) based on their body mass index. Participants were further classified as metabolically healthy or metabolically unhealthy according to the presence of metabolic syndrome (MetS). MetS was defined based on the criteria established by the American Heart Association/National Heart, Lung, and Blood Institute (AHA/NHLBI)[16], requiring the presence of at least three of the following five components: (1) fasting blood glucose ≥ 100 mg/dL or receiving antidiabetic therapy; (2) reduced high-density lipoprotein cholesterol (HDL-C < 40 mg/dL in males or < 50 mg/dL in females) or receiving treatment for low HDL-C; (3) triglycerides ≥ 150 mg/dL or receiving treatment for hypertriglyceridemia; (4) waist circumference ≥ 102 cm in males or ≥ 88 cm in females; or (5) blood pressure ≥ 130/85 mmHg or receiving antihypertensive therapy.

Based on these criteria, the study population was divided into four mutually exclusive groups: metabolically healthy non-obesity (MHNO), metabolically healthy obesity (MHO), metabolically unhealthy non-obesity (MUNO), and metabolically unhealthy obesity (MUO).

Detailed definitions of the MetS-related metabolic health–obesity phenotypes in the CHARLS cohort are provided in **Supplementary Material 3**.

2.4 Exposure and derived indices

The TyG index, TyG-ABSI, and related indices were defined as follows.

(1) $\mathrm{TyG} = \ln\left[\frac{\text{fasting triglycerides (mg/dL)} \times \text{fasting glucose (mg/dL)}}{2}\right]$ [17]

(2) $\mathrm{ABSI} = \frac{\text{WC (m)}}{\text{BMI (kg/m}^2)^{2/3} \times \text{Height (m)}^{1/2}}$ [12]

(3) TyG-ABSI=TyG×ABSI [12]

All other derived indices, including VAI, WHtR, WWI, LAP, BRI, TyG-WC, TyG-BMI, TyG-WHtR, TyG-WWI, TyG-LAP, TyG-VAI, TyG-BRI, ePWV, SII, SIRI, and AISI, were calculated using previously published formulas and are detailed in **Supplementary Material 4**.

2.5 Study outcomes

The outcome variables included all-cause and cardiovascular mortality. Death records were obtained from NHANES-linked publicly available mortality files, which include mortality-related variables specific to adults. The National Death Index provides information on the survival status and causes of death of participants, with data recorded through December 31, 2019. Causes of death were reclassified using the NCHS "113 causes of death" system based on the International Classification of Diseases, 10th Revision (ICD-10). Cardiovascular mortality was determined by the categories "cardiac diseases" (codes 054–068; corresponding to ICD-10 codes I00–I09, I11, I13, and I20–I51) and "cerebrovascular diseases" (code 070; corresponding to ICD-10 codes I60–I69). Non-cardiovascular deaths were treated as competing events in the Fine–Gray subdistribution hazard model.

Detailed definitions of the study outcome in the CHARLS cohort are provided in **Supplementary Material 3**.

2.6 Covariate definitions

In NHANES, covariates including demographic information, lifestyle characteristics, medical history, and current medication use were collected through in-person interviews. Demographic characteristics included age, sex, and race/ethnicity (Mexican American, non-Hispanic Black, non-Hispanic White, other Hispanic, and other races). Socioeconomic factors included education level (< high school, high

157 school, or > high school) and the poverty income ratio (PIR; categorized as ≤ 1.3, 1.3–3.5, or ≥ 3.5).
158 Lifestyle factors included smoking status (never, former, current), alcohol consumption (non-drinker,
159 former, current), and physical activity (MET-minutes/week, continuous). Detailed definitions of smoking
160 and alcohol categories are provided in **Supplementary Material 3**.

161 Clinical comorbidities included: cardiovascular disease (self-reported congestive heart failure, cor-
162 onary artery disease, angina, myocardial infarction, or stroke); hypertension (systolic blood pressure ≥
163 140 mmHg, diastolic blood pressure ≥ 90 mmHg, use of antihypertensive medications, or physician di-
164 agnosis); hyperlipidemia (total cholesterol ≥ 200 mg/dL, triglycerides ≥ 150 mg/dL, LDL-C ≥ 130 mg/dL,
165 HDL-C ≤ 50 mg/dL in women or ≤ 40 mg/dL in men, or use of lipid-lowering therapy); diabetes (fasting
166 blood glucose ≥ 126 mg/dL, HbA1c ≥ 6.5%, or self-reported diagnosis with use of insulin or oral hypo-
167 glycemic agents); chronic kidney disease (CKD; estimated glomerular filtration rate < 60 mL/min/1.73
168 m^2 using the CKD-EPI equation); and cancer (self-reported physician diagnosis). Hypertension, diabetes,
169 CKD, and cancer were recorded as dichotomous variables (yes/no). Medication history included lipid-
170 lowering agents, antihypertensive drugs, and hypoglycemic agents.

171 For exploratory association decomposition analysis, the following biomarkers were additionally
172 considered: estimated pulse wave velocity (ePWV) as an estimate of vascular aging; systemic immune-
173 inflammation index (SII); systemic inflammation response index (SIRI); and aggregate index of systemic
174 inflammation (AISI). Formulas for these indices are provided in **Supplementary Material 4**.

175 Detailed definitions of covariates in the CHARLS cohort are provided in **Supplementary Material**
176 **3**.

177 ## 2.7 Statistical analysis

Missing data were handled using multiple imputation by chained equations (MICE) under the missing at random assumption, generating 10 imputed datasets. Outcome and phenotype variables were included as predictors but not imputed. Continuous variables were imputed using predictive mean matching, and categorical variables using logistic or multinomial logistic regression. Results were pooled using Rubin's rules. Descriptive analyses used weighted means ± standard deviations for continuous variables and weighted percentages with unweighted frequencies for categorical variables. Between-group comparisons used survey-weighted linear regression (F-test) and Rao-Scott corrected chi-square tests. *P*-values were adjusted for multiple comparisons using the Benjamini–Hochberg false discovery rate (FDR) procedure.

Variable selection used the Boruta algorithm (**Figure 3**), and variables with a variance inflation factor ≥ 5 were excluded. Model complexity was controlled by the events per variable principle (≥ 5). Because TyG-ABSI integrates fasting glucose, triglycerides, and body composition, BMI, waist circumference, fasting glucose, and LDL-C were not included to avoid collinearity. Final covariates were age, sex, race/ethnicity, education, poverty income ratio, smoking, alcohol consumption, physical activity, and cancer history.

All analyses incorporated the NHANES complex survey design (sampling weights, SDMVSTRA, SDMVPSU). Multivariable Cox proportional hazards models were constructed with three sequential adjustments: Model 1 unadjusted; Model 2 adjusted for age, sex, and race/ethnicity; Model 3 further adjusted for smoking, alcohol, education, poverty income ratio, cancer, and physical activity. Hazard ratios (HRs) and 95% confidence intervals (CIs) were calculated per 1-SD increment and across quartiles. The proportional hazards assumption was assessed using Schoenfeld residuals.

Restricted cubic spline (RCS) analysis modeled the dose–response relationship using the RCSsci

package, with knots selected across 3–7 candidates (Figure S1). A two-step strategy (at least 10 events per knot; parsimony with $\Delta AIC < 2$) converged to 3 knots across all phenotype groups. Nonlinearity and overall association *P*-values were evaluated.

Competing risk analysis used the Fine–Gray subdistribution hazard model for cardiovascular mortality, treating non-cardiovascular death as a competing event.

Predictive performance was assessed using time-dependent ROC curves at 3, 5, 10, and 15 years, with AUC (c-index) as the metric. The DeLong test compared AUCs, and bootstrap resampling (1,000 iterations) estimated 95% CIs. Incremental predictive value was evaluated using the net reclassification improvement (NRI) and integrated discrimination improvement (IDI), with 1,000 bootstrap iterations, and decision curve analysis (DCA) assessed clinical net benefit.

Subgroup analyses calculated interaction *P*-values for age (< 60 vs ≥ 60 years), sex, smoking, alcohol, chronic kidney disease, cancer history, and use of lipid-lowering, antihypertensive, and hypoglycemic agents.

Sensitivity analyses included: (1) complete-case analysis; (2) E-value analysis; (3) excluding deaths within 2 and 5 years; (4) excluding users of hypoglycemic/lipid-lowering agents, patients with baseline cardiovascular disease, and patients with cancer; (5) excluding advanced CKD (eGFR < 30 mL/min/1.73 m^2) and additional adjustment for eGFR; (6) Fine–Gray competing risk model; and (7) preliminary cross-population comparison in CHARLS.

Effect modification and exploratory association decomposition: To assess whether an ePWV-related vascular aging process modified the TyG-ABSI–mortality association, the population was stratified by ePWV tertiles, with interaction P-values from Wald tests. Three additional interaction models were fitted: TyG-ABSI × age; TyG-ABSI × SBP; and a model including all three interactions (TyG-ABSI × ePWV,

× age, × SBP). Continuous variables were standardized to Z-scores. These analyses were performed within each phenotype (**Table S4**). Exploratory association decomposition (**Table S20**) decomposed the total association into indirect and direct components using the approach of VanderWeele [18]. E-values were calculated using the method of VanderWeele and Ding [19]. Because all candidate mediators (ePWV, SIRI, SII, AISI) were measured at baseline, this analysis is exploratory and does not support causal inference.

Preliminary cross-population comparison in CHARLS (n = 7,239 after exclusions) examined the association between TyG-ABSI and all-cause mortality using MICE, Boruta, multivariable Cox models, and time-dependent ROC curves.

Software: All analyses were performed using R version 4.3.1 (packages: survey, survival, timeROC, RCSsci, mediation, mice). Two-sided $P < 0.05$ was considered statistically significant.

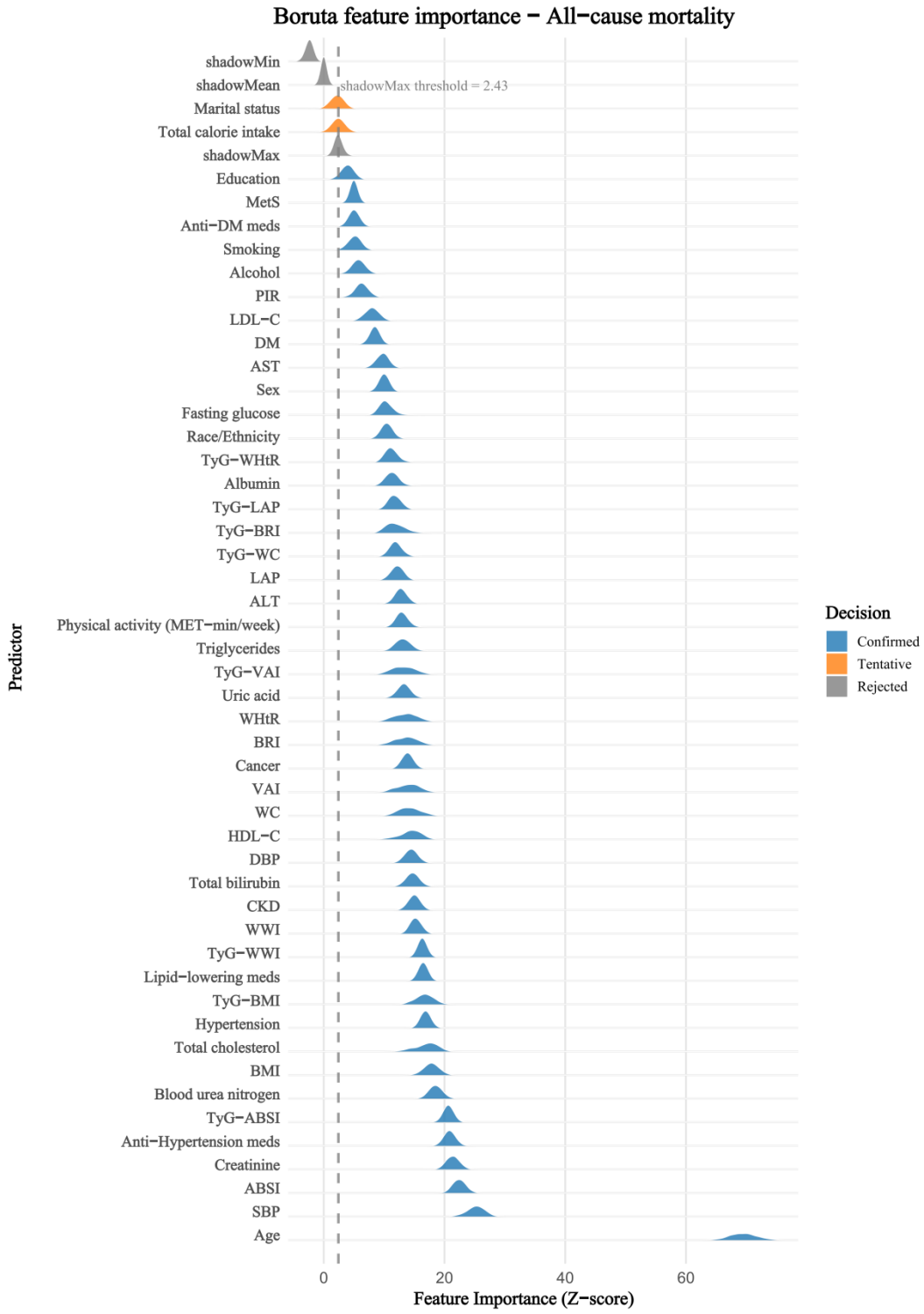


Figure 3. Boruta algorithm feature importance ranking for all-cause mortality. Variables are ordered by Z-score of Mean Decrease in Accuracy. Blue, orange, and gray violin plots denote confirmed features (importance > shadowMax), rejected features, and shadow variables (randomly permuted), respectively. The vertical dashed line indicates the shadowMax threshold. Confirmed variables above this line were retained for multivariate modeling.

3 Results

3.1 Baseline characteristics of study participants

The baseline characteristics of the 20,430 participants in the NHANES cohort, stratified by TyG-ABSI quartiles after exclusion, are shown in **Table 1**. TyG-ABSI quartile distribution exhibited significant sociodemographic and clinical gradients. Higher TyG-ABSI scores were consistently associated with an unfavorable cardiovascular risk profile, characterized by progressively higher prevalences of smoking, comorbidities (including hypertension, diabetes, and chronic kidney disease), and use of antihypertensive and hypoglycemic agents. Notably, both all-cause and cardiovascular mortality increased stepwise across quartiles (both $P < 0.001$). More importantly, the metabolic phenotype distribution underwent a substantial reconfiguration with rising TyG-ABSI: the proportion of MHNO markedly declined, whereas the shares of MUNO and MUO expanded progressively, suggesting that TyG-ABSI captures metabolic health dimensions beyond simple obesity classification.

Table 1. Baseline Characteristics by TyG-ABSI Quartiles

Characteristic	Overall (N = 20,430)	Q1 (N = 5,108)	Q2 (N = 5,107)	Q3 (N = 5,107)	Q4 (N = 5,108)	*P*-value	*P*-adjusted (FDR)
Age, years						< 0.001	< 0.001
Mean ± SD	47.31 ± 18.71	34.64 ± 14.96	44.58 ± 17.35	51.44 ± 17.47	58.60 ± 16.07		
Sex, n (%)						< 0.001	< 0.001
Female	10,065(49.3%)	1,976(38.7%)	2,382(46.6%)	2,810(55.0%)	2,897(56.7%)		
Male	10,365(50.7%)	3,132(61.3%)	2,725(53.4%)	2,297(45.0%)	2,211(43.3%)		
Race/Ethnicity, n (%)						< 0.001	< 0.001
Mexican American	3,869 (18.9%)	727 (14.2%)	959 (18.8%)	1,088(21.3%)	1,095(21.4%)		

Characteristic	Overall (N = 20,430)	Q1 (N = 5,108)	Q2 (N = 5,107)	Q3 (N = 5,107)	Q4 (N = 5,108)	*P*-value	*P*-adjusted (FDR)
Non-Hispanic Black	4,082 (20.0%)	1,773(34.7%)	1,080(21.1%)	714 (14.0%)	515 (10.1%)		
Non-Hispanic White	8,892 (43.5%)	1,755(34.4%)	2,130(41.7%)	2,387(46.7%)	2,620(51.3%)		
Other Hispanic	1,754 (8.6%)	364 (7.1%)	474 (9.3%)	452 (8.9%)	464 (9.1%)		
Other Race - Including Multi-Racial	1,833 (9.0%)	489 (9.6%)	464 (9.1%)	466 (9.1%)	414 (8.1%)		
Marital status, n (%)						< 0.001	< 0.001
Married or living with partner	12,183 (59.6%)	2,508(49.1%)	3,067(60.1%)	3,355(65.7%)	3,253(63.7%)		
Single	8,247 (40.4%)	2,600(50.9%)	2,040(39.9%)	1,752 (34.3%)	1,855(36.3%)		
Poverty income ratio, n (%)						< 0.001	< 0.001
≤ 1.3	6,372 (31.2%)	1,608(31.5%)	1,517(29.7%)	1,501 (29.4%)	1,746(34.2%)		
1.3-3.5	7,787 (38.1%)	1,857(36.4%)	1,911(37.4%)	1,949 (38.2%)	2,070(40.5%)		
≥ 3.5	6,271 (30.7%)	1,643(32.2%)	1,679(32.9%)	1,657 (32.4%)	1,292(25.3%)		
Smoking status, n (%)						< 0.001	< 0.001
Current	4,130 (20.2%)	976 (19.1%)	1,042(20.4%)	1,026 (20.1%)	1,086(21.3%)		
Former	4,900 (24.0%)	738 (14.4%)	1,064(20.8%)	1,402 (27.5%)	1,696(33.2%)		
Never	11,400 (55.8%)	3,394(66.4%)	3,001(58.8%)	2,679 (52.5%)	2,326(45.5%)		
Drinking status, n (%)						< 0.001	< 0.001
Former	3,426 (16.8%)	589 (11.5%)	728 (14.3%)	933 (18.3%)	1,176(23.0%)		
Heavy	4,100 (20.1%)	1,062(20.8%)	1,147(22.5%)	998 (19.5%)	893 (17.5%)		
Mild	6,967 (34.1%)	1,681(32.9%)	1,765(34.6%)	1,814 (35.5%)	1,707(33.4%)		

Characteristic	Overall (N = 20,430)	Q1 (N = 5,108)	Q2 (N = 5,107)	Q3 (N = 5,107)	Q4 (N = 5,108)	*P*-value	*P*-adjusted (FDR)
Moderate	3,036 (14.9%)	1,017(19.9%)	794 (15.5%)	682 (13.4%)	543 (10.6%)		
Never	2,901 (14.2%)	759 (14.9%)	673 (13.2%)	680 (13.3%)	789 (15.4%)		
Hypertension, n (%)						< 0.001	< 0.001
No	12,465 (61.0%)	4,150(81.2%)	3,393(66.4%)	2,836 (55.5%)	2,086(40.8%)		
Yes	7,965 (39.0%)	958 (18.8%)	1,714(33.6%)	2,271 (44.5%)	3,022(59.2%)		
Diabetes mellitus, n (%)						< 0.001	< 0.001
DM	3,424 (16.8%)	159 (3.1%)	408 (8.0%)	813 (15.9%)	2,044(40.0%)		
IFG	1,815 (8.9%)	128 (2.5%)	374 (7.3%)	613 (12.0%)	700 (13.7%)		
IGT	1,194 (5.8%)	154 (3.0%)	286 (5.6%)	412 (8.1%)	342 (6.7%)		
No	13,997 (68.5%)	4,667(91.4%)	4,039(79.1%)	3,269 (64.0%)	2,022(39.6%)		
Chronic kidney disease, n (%)						< 0.001	< 0.001
No	17,200 (84.2%)	4,752(93.0%)	4,537(88.8%)	4,263 (83.5%)	3,648(71.4%)		
Yes	3,230 (15.8%)	356 (7.0%)	570 (11.2%)	844 (16.5%)	1,460(28.6%)		
Cancer history, n (%)						< 0.001	< 0.001
No	18,731 (91.7%)	4,907(96.1%)	4,777(93.5%)	4,620 (90.5%)	4,427(86.7%)		
Yes	1,699 (8.3%)	201 (3.9%)	330 (6.5%)	487 (9.5%)	681 (13.3%)		
Metabolic health and obesity (4 groups), n (%)						< 0.001	< 0.001
MHNO	10,477 (51.3%)	3,849(75.4%)	3,213(62.9%)	2,290 (44.8%)	1,125(22.0%)		
MHO	2,920 (14.3%)	954 (18.7%)	971 (19.0%)	771 (15.1%)	224 (4.4%)		
MUNO	2,734 (13.4%)	28 (0.5%)	255 (5.0%)	715 (14.0%)	1,736(34.0%)		

Characteristic	Overall (N = 20,430)	Q1 (N = 5,108)	Q2 (N = 5,107)	Q3 (N = 5,107)	Q4 (N = 5,108)	*P*-value	*P*-adjusted (FDR)
MUO	4,299 (21.0%)	277 (5.4%)	668 (13.1%)	1,331 (26.1%)	2,023(39.6%)		
Body mass index, kg/m²						< 0.001	< 0.001
Mean ± SD	28.80 ± 6.51	26.90 ± 6.73	28.51 ± 6.60	29.65 ± 6.23	30.16 ± 5.98		
Waist circumference, cm						< 0.001	< 0.001
Mean ± SD	98.16 ± 15.93	87.39 ± 13.81	95.91 ± 14.40	102.09 ± 14.07	107.24 ±14.13		
Diastolic blood pressure, mmHg						< 0.001	< 0.001
Mean ± SD	70.15 ± 11.24	67.67 ± 10.43	70.34 ± 10.85	71.47 ± 11.29	71.12 ± 11.93		
Systolic blood pressure, mmHg						< 0.001	< 0.001
Mean ± SD	123.27 ± 18.66	115.69 ± 14.88	121.49 ± 17.58	125.71 ± 18.58	130.19 ± 20.06		
Total calorie intake, kcal/day						0.010	0.010
Mean ± SD	2,007.71 ± 966.41	2,042.56 ± 980.86	2,012.38 ± 933.06	2,039.03 ± 1,008.10	1,936.90 ± 938.18		
Physical activity, MET-min/week						< 0.001	< 0.001
Mean ± SD	2,606.73 ± 5,227.27	3,220.15 ± 5,935.75	2,882.18 ± 5,520.89	2,422.63 ± 4,903.57	1,901.90 ± 4,309.41		
Triglycerides, mg/dL						< 0.001	< 0.001
Mean ± SD	120.16 ± 67.07	64.61 ± 24.73	96.78 ± 35.58	129.40 ± 47.50	189.86 ± 72.69		
Total cholesterol, mg/dL						< 0.001	< 0.001
Mean ± SD	192.42 ± 40.77	174.57 ± 34.52	191.88 ± 37.11	198.60 ± 39.83	204.62 ± 44.59		
HDL cholesterol,						< 0.001	< 0.001

Characteristic	Overall (N = 20,430)	Q1 (N = 5,108)	Q2 (N = 5,107)	Q3 (N = 5,107)	Q4 (N = 5,108)	*P*-value	*P*-adjusted (FDR)
mg/dL							
Mean ± SD	53.44 ± 15.39	59.76 ± 15.71	55.88 ± 15.21	51.34 ± 14.23	46.78 ± 13.14		
LDL cholesterol, mg/dL						< 0.001	< 0.001
Mean ± SD	114.91 ± 35.50	101.40±29.52	116.48±33.36	121.39±35.44	120.36±39.30		
Albumin, g/L						< 0.001	< 0.001
Mean ± SD	42.37 ± 3.41	42.83 ± 3.38	42.47 ± 3.43	42.24 ± 3.33	41.93 ± 3.43		
ALT, U/L						< 0.001	< 0.001
Mean ± SD	25.28 ± 27.86	21.37 ± 34.94	24.44 ± 19.23	27.31 ± 20.10	27.99 ± 32.90		
Total bilirubin, μmol/L						0.295	0.295
Mean ± SD	11.98 ± 5.34	12.05 ± 5.69	11.94 ± 5.44	12.07 ± 5.28	11.84 ± 4.93		
Blood urea nitrogen, mg/dL						< 0.001	< 0.001
Mean ± SD	13.34 ± 5.55	12.00 ± 4.20	12.88 ± 4.78	13.69 ± 5.74	14.80 ± 6.77		
Uric acid, mg/dL						< 0.001	< 0.001
Mean ± SD	5.46 ± 1.42	4.92 ± 1.25	5.34 ± 1.32	5.69 ± 1.40	5.91 ± 1.49		
Creatinine, μmol/L						< 0.001	< 0.001
Mean ± SD	77.01 ± 35.56	73.39 ± 25.07	75.77 ± 39.77	78.11 ± 38.80	80.78 ± 36.24		
Fasting glucose, mg/dL						< 0.001	< 0.001
Mean ± SD	105.98 ± 31.44	93.26 ± 9.90	98.66 ± 13.61	104.95 ± 21.27	127.07 ± 50.57		
Antihypertensive medication, n (%)						< 0.001	< 0.001
No	12,769 (62.5%)	4,288(83.9%)	3,520(68.9%)	2,934 (57.5%)	2,027(39.7%)		
Yes	7,661 (37.5%)	820 (16.1%)	1,587(31.1%)	2,173 (42.5%)	3,081(60.3%)		

Characteristic	Overall (N = 20,430)	Q1 (N = 5,108)	Q2 (N = 5,107)	Q3 (N = 5,107)	Q4 (N = 5,108)	*P*-value	*P*-adjusted (FDR)
Lipid-lowering medication, n (%)						< 0.001	< 0.001
No	14,322 (70.1%)	4,667(91.4%)	3,967(77.7%)	3,321 (65.0%)	2,367(46.3%)		
Yes	6,108 (29.9%)	441 (8.6%)	1,140(22.3%)	1,786 (35.0%)	2,741(53.7%)		
Antidiabetic medication, n (%)						< 0.001	< 0.001
No	16,710 (81.8%)	4,699(92.0%)	4,441(87.0%)	4,181 (81.9%)	3,389(66.3%)		
Yes	3,720 (18.2%)	409 (8.0%)	666 (13.0%)	926 (18.1%)	1,719(33.7%)		
Cardiovascular mortality, n (%)						< 0.001	< 0.001
No	19,656 (96.2%)	5,071(99.3%)	4,988(97.7%)	4,876 (95.5%)	4,721(92.4%)		
Yes	774 (3.8%)	37 (0.7%)	119 (2.3%)	231 (4.5%)	387 (7.6%)		
All-cause mortality, n (%)						< 0.001	< 0.001
No	17,906 (87.6%)	4,946(96.8%)	4,687(91.8%)	4,412 (86.4%)	3,861(75.6%)		
Yes	2,524 (12.4%)	162 (3.2%)	420 (8.2%)	695 (13.6%)	1,247(24.4%)		

Data are n (%) unless otherwise indicated.

Continuous variables: weighted mean ± SD; Categorical variables: weighted percentages (unweighted frequencies). *P*-values: continuous - survey-weighted linear regression (F-test); categorical - survey-weighted chi-square (Rao-Scott). *P*-values adjusted by FDR (Benjamini-Hochberg). Groups: Q1 (lowest TyG-ABSI) to Q4 (highest TyG-ABSI). Abbreviations: TyG-ABSI = TyG-ABSI = triglyceride-glucose index × A Body Shape Index; MHNO = metabolically healthy non-obese; MHO = metabolically healthy obese; MUNO = metabolically unhealthy non-obese; MUO = metabolically unhealthy obese; CVD = cardiovascular disease; CKD = chronic kidney disease; BMI = body mass index; HDL = high-density lipoprotein; LDL = low-density lipoprotein; ALT = alanine aminotransferase; DM, diabetes mellitus; IFG, impaired fasting glucose; IGT, impaired glucose tolerance.

3.2 Association between TyG-ABSI and mortality risk

Cox regression results for the association between TyG-ABSI and mortality risk are shown in **Table S1** (overall and by phenotype).

Overall population: A significant association driven by the metabolically unhealthy subgroup. In

Model 3, each additional standard deviation increased the all-cause mortality risk by 19% (HR = 1.19; 95% CI: 1.12–1.25; $P < 0.001$) and the cardiovascular mortality risk by 27% (HR = 1.27; 95% CI: 1.14–1.41; $P < 0.001$). The quartile trend test was significant (P trend < 0.001): the HR for all-cause mortality was 1.57 (1.28–1.92) and for cardiovascular mortality was 1.77 (1.17–2.68; $P = 0.007$) between Q4 and Q1.

Metabolic Unhealthy Phenotypes (MUNO and MUO): robust linear associations were observed. The TyG-ABSI association was the strongest and most consistent among individuals with metabolic unhealthy phenotypes. For every one standard deviation increase in the MUNO group, the all-cause mortality risk increased by 27% (HR = 1.27; 95% CI: 1.12–1.44; $P < 0.001$), and the cardiovascular mortality risk increased by 49% (HR = 1.49; 95% CI: 1.17– 1.89; $P = 0.001$). Corresponding HR values in the MUO group were 1.22 (95% CI: 1.08–1.38; $P = 0.002$) and 1.33 (95% CI: 1.07–1.64; $P = 0.009$), respectively. Both groups exhibited significant positive dose-response trends (P trend < 0.05).

Metabolic Health Non-Obesity (MHNO): A significant but attenuated association. For every one standard deviation increase, the all-cause mortality risk rises by 15% (HR = 1.15, 95% CI: 1.03–1.28, $P = 0.012$), with a significant linear trend (P trend = 0.034). The estimated hazard ratio for cardiovascular mortality was not statistically significant (HR = 1.18, 95% CI: 0.96–1.45, $P = 0.116$), but a quartile-based linear trend remained significant (P trend = 0.024).

Metabolic Health Obesity (MHO): TyG-ABSI showed no statistically significant association with all-cause mortality (HR = 0.99, 95% CI: 0.77–1.27, $P = 0.950$) or cardiovascular mortality (HR = 1.36, 95% CI: 0.86–2.16, $P = 0.186$), and linear trend tests were not significant (P trend = 0.622 and 0.717, respectively). However, the cardiovascular mortality estimate was positive with a wide confidence inter-

val, so a clinically relevant association cannot be excluded. With 205 all-cause deaths and 62 cardiovascular deaths, the MHO subgroup had limited statistical power. Under Model 3 with multiple covariates and complex survey weighting, the study was underpowered to detect modest associations (roughly HR < 1.8–2.0 for cardiovascular mortality). Therefore, this null result should be interpreted with caution.This range was approximated from the observed event count and the standard error of log(HR) in the fully adjusted model, and should be considered a conservative estimate rather than a precise power calculation. This pattern remained consistent across sensitivity analyses.

3.3 Restrictive Cubic Spline Analysis

Restricted cubic spline (RCS) analysis (**Figure 4**) illustrates the dose–response relationships between TyG-ABSI and all-cause and cardiovascular mortality.

In the overall population (panels A and F), TyG-ABSI exhibited a significant nonlinear dose–response relationship with both outcomes (overall $P < 0.001$; nonlinear $P < 0.001$). Risk increased progressively with a steep upward slope at high TyG-ABSI levels, without evidence of a safe threshold.

In metabolically unhealthy phenotypes, both MUNO (panels D and I) and MUO (panels E and J) showed linear associations (nonlinear $P > 0.05$). The hazard ratios increased continuously across the observed range without distinct inflection points, indicating a stable dose–response relationship.

The MHNO group (panels B and G) exhibited significant nonlinearity in both all-cause and cardiovascular mortality (nonlinear $P < 0.001$). The all-cause mortality curve showed a potential threshold-like pattern around a Z-score of approximately 2.1 (TyG-ABSI ≈ 0.86). This threshold was hypothesis-generating and should be interpreted as a region rather than a precise cut-point, with the risk rising gradually before accelerating significantly thereafter, reaching a peak hazard ratio (HR) of 2.70 (95% CI: 1.99–3.66); the cardiovascular mortality curve continued to accelerate throughout the observation period,

achieving an HR of 3.5 near Z-score ≈ 3.0 (TyG-ABSI ≈ 0.927). This nonlinear pattern suggests that extremely high levels of TyG-ABSI in the MHNO population may exceed a hypothesis-generating threshold of metabolic compensation.

In the MHO group (panels C and H), no significant nonlinearity was detected (all-cause P = 0.229; cardiovascular P = 0.072). Curves fluctuated around HR = 1 with wide confidence intervals, consistent with the Cox regression finding of no significant association.

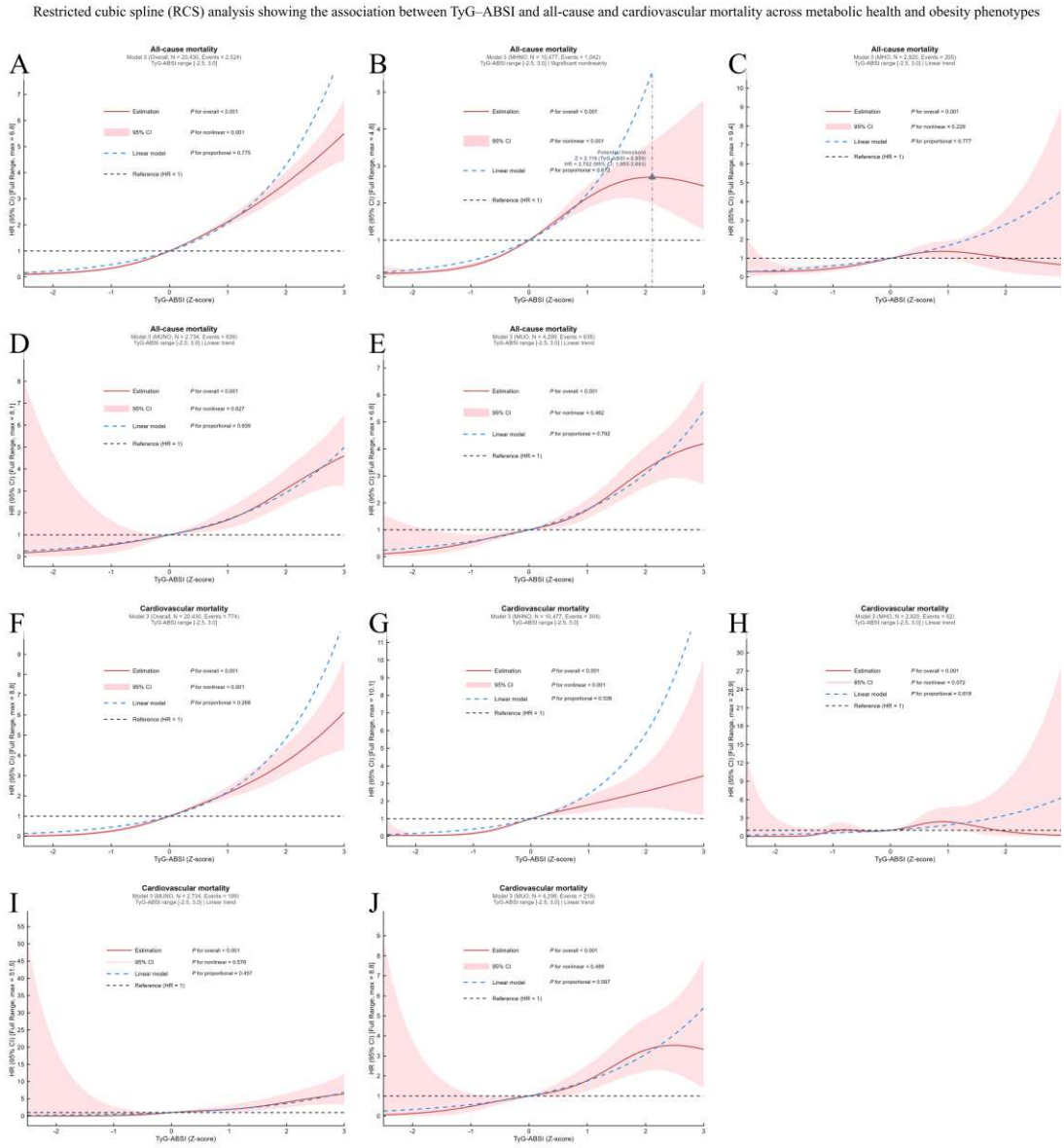


Figure 4. Restricted cubic spline (RCS) analysis showing the association between TyG-ABSI and all-cause and cardiovascular mortality across metabolic health and obesity phenotypes. Panels A–E show all-cause mortality for Total, MHNO, MHO, MUNO, and MUO groups, respectively; panels F–J show cardiovascular mortality for the same groups. The solid lines represent hazard ratios, and shaded areas indicate 95% confidence intervals.

3.4 Kaplan-Meier Analysis

Kaplan-Meier analysis (**Figure 5**) showed that after stratification by TyG-ABSI quartiles, cumulative risk curves for the overall population and the MHNO, MUNO, and MUO subgroups were significantly separated (all log-rank $P < 0.001$). In the MHO subgroup, although the curve showed nominal

303 separation (log-rank $P < 0.001$), the 20-year absolute mortality risk in Q4 remained low, and multivaria-
304 ble Cox regression confirmed no independent association (**Table S1**), suggesting that this separation
305 reflected confounding by age and comorbidities rather than a genuine effect of TyG-ABSI.

306 The metabolically unhealthy phenotypes (MUNO and MUO) had the highest absolute mortality
307 risks, with the 20-year cumulative all-cause mortality risk in Q4 of the MUO subgroup approaching
308 1.0. Even within the metabolically healthy group, the Q4 cumulative risk in MHNO was approximately
309 7.5 times that of Q1. For cardiovascular mortality, significant separation was observed in the overall
310 population and the MHNO, MUNO, and MUO subgroups (all log-rank $P < 0.001$), whereas separation
311 in MHO was weaker (log-rank $P = 0.007$). These results suggest that the association between TyG-ABSI
312 and mortality is present across phenotypes, but the absolute risk burden is more pronounced in metabol-
313 ically unhealthy populations.

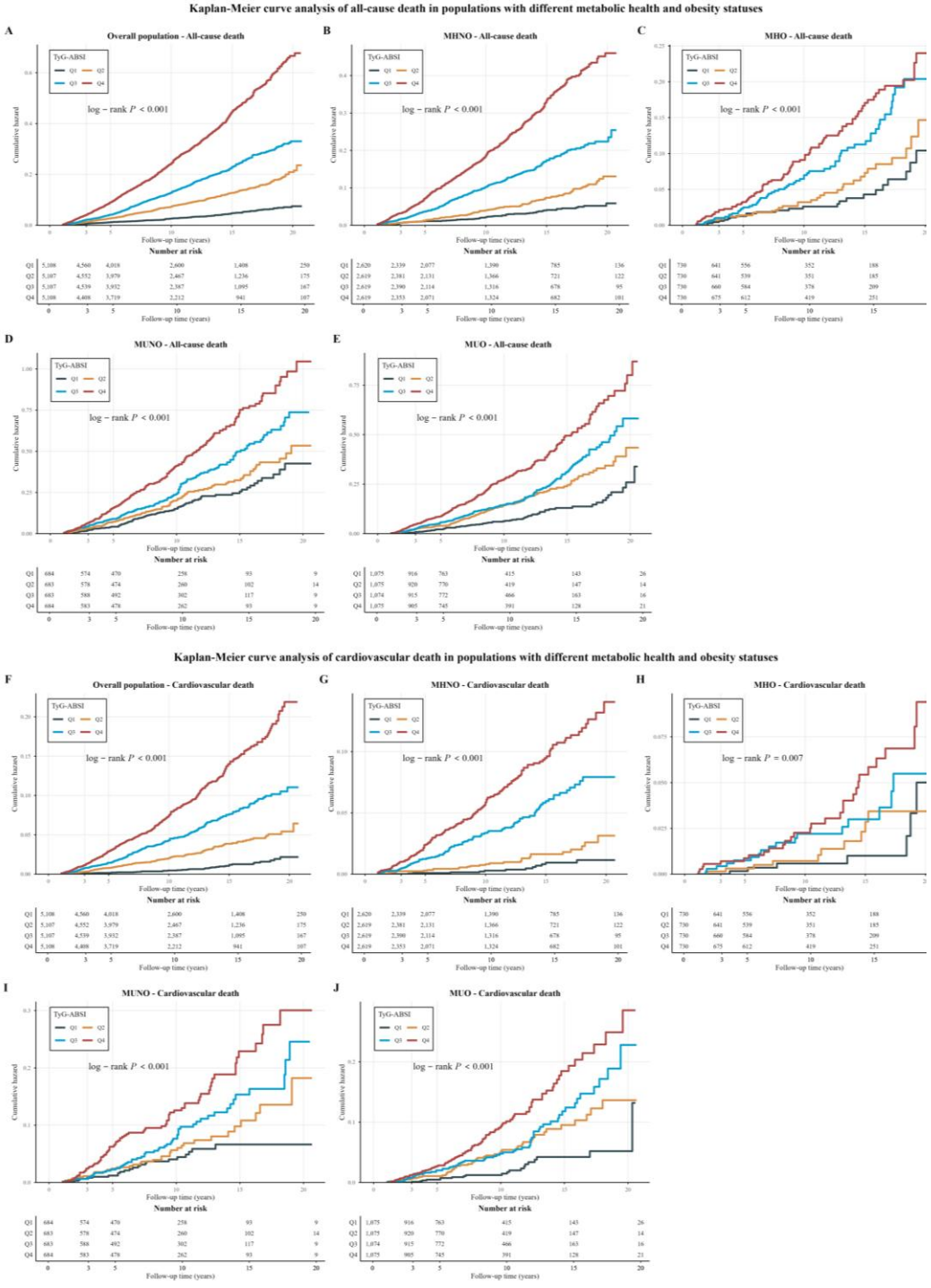


Figure 5. Kaplan-Meier survival curves for all-cause and cardiovascular mortality according to TyG-ABSI quartiles across different metabolic health and obesity statuses.

(A–E) Kaplan-Meier curve analysis of all-cause death: (A) overall population; (B) metabolically healthy non-obese (MHNO) population; (C) metabolically healthy obese (MHO) population; (D)

metabolically unhealthy non-obese (MUNO) population; (E) metabolically unhealthy obese (MUO) population. (F–J) Kaplan-Meier curve analysis of cardiovascular death: (F) overall population; (G) MHNO population; (H) MHO population; (I) MUNO population; (J) MUO population. Curves are stratified by TyG-ABSI quartiles (Q1–Q4, with Q1 as the lowest quartile and Q4 as the highest). The numbers of participants at risk at each follow-up time point are shown below each panel. Between-group differences were assessed using the log-rank test, and the corresponding P values are presented in the figure.

3.5 Prediction Performance Comparison

Time-dependent ROC analysis of predictive performance demonstrated that in the overall population (**Figure 6**), TyG-ABSI exhibited time-dependent discriminative capacity for both all-cause mortality and cardiovascular mortality, consistently outperforming the random classifier at all time points (AUC > 0.5).

In the metabolic health and obesity phenotype subgroups (**Figures S3** and **S4**), predictive performance showed marked heterogeneity. For all-cause mortality, discriminative capacity was strongest in the MHNO group (**Figure S3A**, 15-year AUC = 0.717), modest in the MUNO group (**Figure S3C**, AUC range 0.623–0.657) and MUO group (**Figure S3D**, 3-year AUC = 0.690), and weakest in the MHO group (**Figure S3B**, AUC ≤ 0.626). A similar pattern was observed for cardiovascular mortality (**Figure S4**): the MHNO (panel A) and MUO (panel D) groups exhibited superior performance relative to the MHO (panel B) and MUNO (panel C) groups. In contrast, TyG-BMI and TyG-VAI showed poor discriminative ability across all subgroups, approaching that of random classifiers (AUC ≈ 0.500).

The heat map (**Figure S5**) and c-index line plot (**Figure S6**) visually present the discriminant capacity matrices of each indicator across phenotypes and follow-up time points. TyG-ABSI maintained the highest AUC values across most phenotypes and time points, with performance improving over time. In the overall population, TyG-ABSI achieved 15-year AUCs of 0.734 for all-cause mortality and 0.748 for cardiovascular mortality, outperforming TyG-WWI (0.717) and other competing indices. However,

in the MHO phenotype, the advantage of TyG-ABSI for cardiovascular mortality prediction was substantially attenuated: TyG-WWI showed marginally higher values at early time points, TyG-BRI was superior at 10 years, and by 15 years TyG-ABSI and TyG-WWI converged to similar levels. This convergence suggests that in the MHO phenotype, body composition-based indices alone may capture prognostic information comparable to—or even exceeding—that of TyG-ABSI, raising questions about the added value of incorporating metabolic data in this specific subgroup.

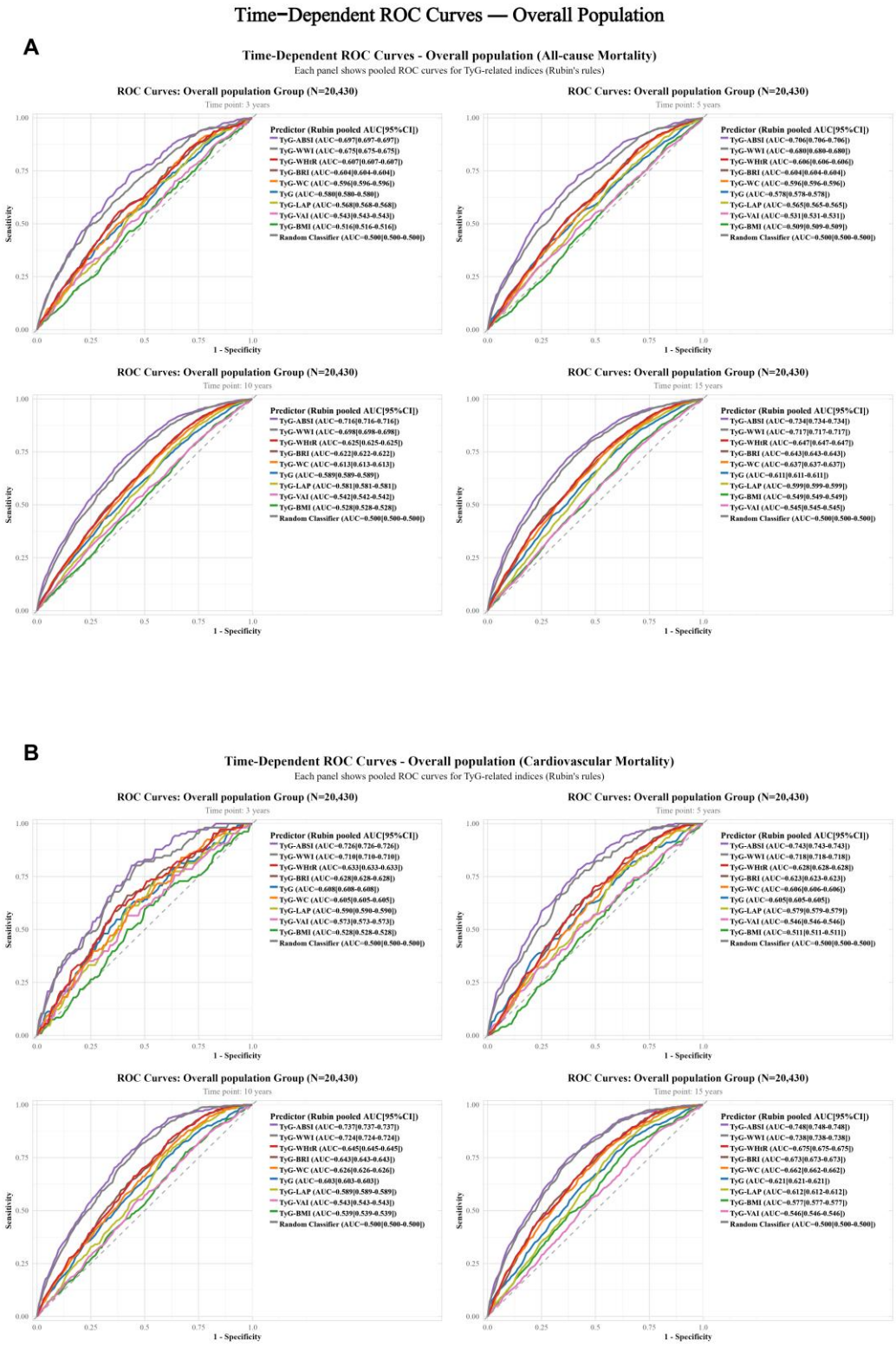


Figure 6. Time-dependent ROC curves for TyG-related indices in the overall population (N = 20,430). (A) All-cause mortality at 3, 5, 10, and 15 years; (B) Cardiovascular mortality at 3, 5, 10, and 15 years.

AUC values were pooled across 10 multiple imputation datasets using Rubin's rules. The dashed diagonal line represents the random classifier (AUC = 0.500).

3.6 Incremental prediction value and clinical utility

To evaluate the incremental predictive value of TyG-ABSI, we calculated NRI and IDI across three sequentially defined models. **Basic model 1** comprised the Framingham Risk Score variables (age group, sex, total cholesterol, HDL-C, smoking, systolic blood pressure, diabetes, and antihypertensive medication use). **Basic model 2** comprised the ASCVD pooled cohort equations (PCE) variables (age group, sex, race/ethnicity, total cholesterol, HDL-C, smoking, systolic blood pressure, diabetes, and antihypertensive medication use). **Basic model 3** adjusted for age group, sex, race/ethnicity, smoking, drinking, education, poverty income ratio (PIR), cancer history, and physical activity.

As shown in **Supplementary Table 2**, incorporating TyG-ABSI into **Basic model 3** significantly improved discriminative accuracy for all-cause mortality (IDI = 0.194, 95% CI 0.119–0.257, $P < 0.001$) and cardiovascular mortality (IDI = 0.258, 95% CI 0.152–0.360, $P < 0.001$) in the overall population. Similar improvements were observed when TyG-ABSI was added to **Basic models 1** and **2** (all $P < 0.05$). In contrast, NRI values in **Basic model 3** were small and not statistically significant (all-cause NRI = 0.004, $P = 0.222$; cardiovascular NRI = 0.007, $P = 0.140$). This divergence suggests that TyG-ABSI improves the granularity of continuous risk estimation rather than reclassifying individuals across conventional risk thresholds.

In phenotype-stratified analyses using **Basic model 3**, significant incremental value was observed for all-cause mortality in MUO (IDI = 0.207, $P = 0.001$) and for cardiovascular mortality in MUNO (IDI = 0.281, $P = 0.009$), MUO (IDI = 0.231, $P = 0.034$), and MHNO (IDI = 0.204, $P = 0.040$). No significant incremental value was detected in MHO for either outcome (all-cause IDI = 0.012, $P = 0.909$; cardiovascular IDI = 0.229, $P = 0.359$). Because IDI magnitude is influenced by event rate, we emphasize the

presence or absence of statistical significance rather than ranking absolute IDI values.

Decision curve analysis (DCA) showed that, in the overall population, the TyG-ABSI model based on **Basic model 3** yielded higher net benefits than other TyG-derived metrics and treat-all/none strategies within the low-to-medium risk threshold range (approximately 5%–25%) (**Figure S7)**. In MUNO and MUO, net benefit was superior (**Figures S10–S11**), whereas in MHO the curves nearly overlapped, indicating limited clinical decision-making value (**Figure S9**).

3.7 Subgroup analysis

Subgroup analysis showed that associations of TyG-ABSI with all-cause and cardiovascular mortality were directionally consistent (HR > 1) in most metabolically unhealthy subgroups, whereas no significant association was observed in MHO. All interaction *P*-values were adjusted for multiple comparisons using the Benjamini–Hochberg false discovery rate (FDR) method; FDR-adjusted interaction *P*-values are presented in **Figure 7** and **Figures S12–S15**. In the overall population, interactions remained significant after FDR correction for sex, poverty-income ratio, smoking, alcohol consumption, chronic kidney disease, cancer history, and use of antihypertensive and glucose-lowering medications; the interaction with age was borderline.

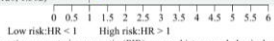
Phenotype-stratified analyses further revealed key heterogeneities (**Figures S12–S15**). The modifying effect of age on TyG-ABSI was observed only in metabolically unhealthy individuals (MUNO: $P < 0.001$ for all-cause mortality; MUO: $P = 0.020$ for cardiovascular mortality), whereas no significant interaction was detected in metabolically healthy phenotypes. Notably, in MHO, cancer history significantly modified the effect of TyG-ABSI (P for interaction = 0.002), suggesting that the predictive value of TyG-ABSI may be overshadowed by cancer-related risk when malignancy is present.

In MHO, most subgroup interactions were not statistically significant after FDR correction (**Figure**

381 **S13**), further supporting limited evidence for TyG-ABSI utility in this phenotype. In contrast, MUO ex-
382 hibited the most extensive significant interactions, involving PIR, smoking, CKD, and use of antihyper-
383 tensive or glucose-lowering medications, indicating that metabolically unhealthy obese individuals may
384 represent an important target population for TyG-ABSI prediction (**Figure S15**).

A: TyG-ABSI and Overall All-Cause Mortality

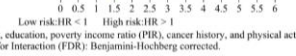
Variable	Participants	HR (95% CI)	*P* value	*P* for Interaction	*P* for Interaction (FDR)
Age				0.045	0.050
< 60	533/14,139 (3.8%)	1.417 (1.281, 1.568)	< 0.001		
≥ 60	1,991/6,291 (31.6%)	1.159 (1.097, 1.226)	< 0.001		
Gender				< 0.001	< 0.001
Female	1,442/10,065 (14.3%)	1.176 (1.098, 1.260)	< 0.001		
Male	1,082/10,365 (10.4%)	1.189 (1.110, 1.275)	< 0.001		
Poverty income ratio, n (%)				< 0.001	< 0.001
≤ 1.3	829/6,334 (13.1%)	1.166 (1.071, 1.268)	< 0.001		
1.3-3.5	1,101/7,747 (14.2%)	1.207 (1.118, 1.303)	< 0.001		
≥ 3.5	594/6,349 (9.4%)	1.195 (1.072, 1.332)	0.001		
Smoking status, n (%)				< 0.001	< 0.001
Current	533/4,099 (13.0%)	1.180 (1.063, 1.310)	0.002		
Former	977/4,912 (19.9%)	1.210 (1.116, 1.312)	< 0.001		
Never	1,014/11,419 (8.9%)	1.187 (1.099, 1.281)	< 0.001		
Drinking status, n (%)				< 0.001	< 0.001
former	798/3,415 (23.4%)	1.184 (1.086, 1.291)	< 0.001		
heavy	290/4,087 (7.1%)	1.295 (1.117, 1.501)	< 0.001		
mild	817/6,960 (11.7%)	1.125 (1.027, 1.232)	0.011		
moderate	226/3,044 (7.4%)	1.161 (0.980, 1.376)	0.085		
never	393/2,924 (13.4%)	1.295 (1.146, 1.464)	< 0.001		
Chronic kidney disease, n (%)				< 0.001	< 0.001
No	1,429/17,195 (8.3%)	1.131 (1.059, 1.208)	< 0.001		
Yes	1,095/3,235 (33.8%)	1.182 (1.098, 1.273)	< 0.001		
Cancer history, n (%)				< 0.001	< 0.001
No	1,997/18,733 (10.7%)	1.231 (1.166, 1.299)	< 0.001		
Yes	527/1,697 (31.1%)	1.007 (0.898, 1.128)	0.907		
Lipid-lowering medication, n (%)				0.165	0.165
No	901/14,279 (6.3%)	1.185 (1.084, 1.295)	< 0.001		
Yes	1,623/6,151 (26.4%)	1.195 (1.121, 1.274)	< 0.001		
Antihypertensive medication, n (%)				< 0.001	< 0.001
No	685/12,771 (5.4%)	1.190 (1.077, 1.315)	< 0.001		
Yes	1,839/7,659 (24.0%)	1.177 (1.111, 1.248)	< 0.001		
Antidiabetic medication, n (%)				0.002	0.003
No	1,723/16,682 (10.3%)	1.138 (1.064, 1.217)	< 0.001		
Yes	801/3,748 (21.4%)	1.235 (1.120, 1.362)	< 0.001		



Model 3: Adjusted for age, gender, race/ethnicity, smoking, drinking, education, poverty income ratio (PIR), cancer history, and physical activity (MET-min/week). TyG-ABSI standardized (Z-score) to HR per 1-SD increment. *P* for Interaction: raw *P* values; *P* for Interaction (FDR): Benjamini-Hochberg corrected.

B: TyG-ABSI and Overall CVD Mortality

Variable	Participants	HR (95% CI)	*P* value	*P* for Interaction	*P* for Interaction (FDR)
Age				0.003	0.005
< 60	127/14,139 (0.9%)	1.854 (1.518, 2.263)	< 0.001		
≥ 60	647/6,291 (10.3%)	1.202 (1.090, 1.325)	< 0.001		
Gender				< 0.001	< 0.001
Female	456/10,065 (4.5%)	1.182 (1.045, 1.336)	0.008		
Male	318/10,365 (3.1%)	1.350 (1.190, 1.532)	< 0.001		
Poverty income ratio, n (%)				< 0.001	< 0.001
≤ 1.3	252/6,334 (4.0%)	1.222 (1.051, 1.419)	0.009		
1.3-3.5	347/7,747 (4.5%)	1.283 (1.115, 1.477)	< 0.001		
≥ 3.5	175/6,349 (2.8%)	1.357 (1.103, 1.670)	0.004		
Smoking status, n (%)				< 0.001	< 0.001
Current	128/4,099 (3.1%)	1.192 (0.965, 1.473)	0.104		
Former	297/4,912 (6.0%)	1.442 (1.245, 1.671)	< 0.001		
Never	349/11,419 (3.1%)	1.194 (1.047, 1.362)	0.008		
Drinking status, n (%)				0.335	0.335
former	244/3,415 (7.1%)	1.302 (1.115, 1.521)	< 0.001		
heavy	69/4,087 (1.7%)	1.276 (0.941, 1.731)	0.117		
mild	262/6,960 (3.8%)	1.190 (1.014, 1.396)	0.033		
moderate	63/3,044 (2.1%)	1.389 (0.968, 1.992)	0.073		
never	136/2,924 (4.7%)	1.256 (1.022, 1.544)	0.031		
Chronic kidney disease, n (%)				< 0.001	< 0.001
No	385/17,195 (2.2%)	1.194 (1.052, 1.355)	0.006		
Yes	389/3,235 (12.0%)	1.231 (1.087, 1.395)	0.001		
Cancer history, n (%)				0.109	0.122
No	648/18,733 (3.5%)	1.297 (1.180, 1.426)	< 0.001		
Yes	126/1,697 (7.4%)	1.132 (0.893, 1.434)	0.305		
Lipid-lowering medication, n (%)				0.006	0.009
No	225/14,279 (1.6%)	1.275 (1.053, 1.542)	0.012		
Yes	549/6,151 (8.9%)	1.237 (1.105, 1.385)	< 0.001		
Antihypertensive medication, n (%)				< 0.001	< 0.001
No	157/12,771 (1.2%)	1.307 (1.057, 1.617)	0.013		
Yes	617/7,659 (8.1%)	1.233 (1.114, 1.365)	< 0.001		
Antidiabetic medication, n (%)				0.010	0.013
No	509/16,682 (3.1%)	1.187 (1.049, 1.344)	0.007		
Yes	265/3,748 (7.1%)	1.325 (1.113, 1.577)	0.001		



Model 3: Adjusted for age, gender, race/ethnicity, smoking, drinking, education, poverty income ratio (PIR), cancer history, and physical activity (MET-min/week). TyG-ABSI standardized (Z-score) to HR per 1-SD increment. *P* for Interaction: raw *P* values; *P* for Interaction (FDR): Benjamini-Hochberg corrected.

Figure 7. Subgroup analysis of TyG-ABSI with mortality risk in the overall population.

All HRs were derived from Model 3, which was adjusted for the following covariates: age, sex, poverty-income ratio, smoking status, alcohol consumption, chronic kidney disease (CKD), history of cancer, use of lipid-lowering agents, use of glucose-lowering agents, and use of antihypertensive medications.*P*-values for interaction were obtained from likelihood-ratio tests comparing models with and without the TyG-ABSI × subgroup interaction terms, and were pooled across 10 multiply imputed datasets using Rubin's rules.

3.8 Effect modification of ePWV-stratified analysis and preliminary association decomposition analysis

Stratified analyses by estimated pulse wave velocity (ePWV) tertiles were performed within each metabolic health–obesity phenotype using Model 3 (**Table S3**).

In the overall population, ePWV significantly modified the TyG-ABSI–mortality association (P for interaction = 0.006 for all-cause; 0.004 for cardiovascular mortality), with effect estimates increasing then declining across tertiles. The interaction was most evident in MUO (P for interaction = 0.022 for all-cause; 0.027 for cardiovascular mortality). For all-cause mortality, the association was significant in the highest ePWV tertile (HR = 1.19, 95% CI 1.04–1.36) and borderline in T2, but not in T1.

In contrast, in the MHO phenotype, no statistically significant TyG-ABSI × ePWV interaction was observed for either outcome (*P* for interaction = 0.769 for all-cause mortality), consistent with the overall null finding in MHO. In the MUNO phenotype, HRs were elevated across strata but the interaction was not significant (*P* for interaction = 0.549 for all-cause mortality). In the MHNO phenotype, the interaction was also not significant (*P* for interaction = 0.28 for all-cause mortality).

To assess whether this interaction was independent of age or SBP, additional interaction models were fitted (**Table S4**). In MUO, the TyG-ABSI × ePWV interaction was significant for both outcomes before adjustment (all-cause: HR = 0.79, $P < 0.001$; cardiovascular: HR = 0.72, $P = 0.005$), but after

simultaneous adjustment for TyG-ABSI × age and TyG-ABSI × SBP, it was no longer statistically significant (all-cause: HR = 0.73, $P = 0.197$; cardiovascular: HR = 1.68, $P = 0.239$). These findings suggest that the apparent effect modification by ePWV in MUO may partly reflect age- or SBP-related interactions. No significant TyG-ABSI × ePWV interaction was observed in MHO or MUNO before or after adjustment (all $P > 0.05$).

Exploratory association decomposition analysis (**Table S20**; **Figure 8**) estimated the proportion of the total association accounted for by indirect components (overall: 57.4% for all-cause, 54.4% for cardiovascular mortality; MUO: 29.5% and 31.1%, respectively). E-values for total effects were 3.03 and 3.37, suggesting moderate robustness to unmeasured confounding. Because ePWV and TyG-ABSI were measured at the same baseline time point, this analysis is exploratory and does not support causal inference. Systemic inflammatory markers (SIRI, SII, AISI) showed minimal associations (explained proportions ≤ 7%), suggesting that systemic inflammation is unlikely to be a primary mechanism.

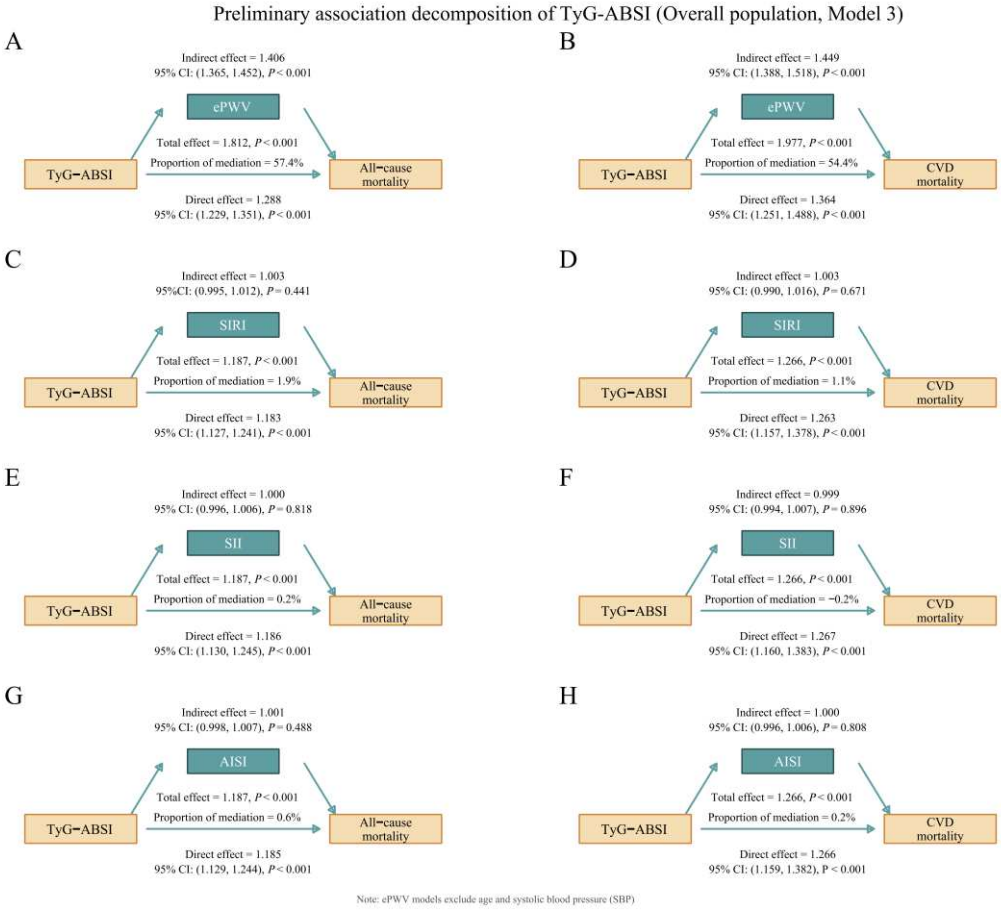


Figure 8. Preliminary association decomposition of TyG-ABSI with all-cause and cardiovascular mortality in the overall population (Model 3).

Panels (A, C, E, G) show results for all-cause mortality; panels (B, D, F, H) show results for cardiovascular mortality. Candidate intermediate variables are: (A–B) estimated pulse wave velocity (ePWV); (C–D) systemic inflammation response index (SIRI); (E–F) systemic immune-inflammation index (SII); (G–H) aggregate index of systemic inflammation (AISI). Numbers along arrows represent hazard ratios (HR). Total, indirect, and direct associations are presented with 95% confidence intervals and *P* values. The proportion of association explained is the percentage of the total association accounted for by the indirect association. Model 3 adjusted for age, sex, race/ethnicity, cancer, smoking, educational level, alcohol consumption, physical activity, and income-to-poverty ratio; for ePWV models, age and systolic blood pressure (SBP) were excluded because both are components of the ePWV calculation formula. These proportions are preliminary and should not be interpreted as causal mediation effects.

3.9 Sensitivity Analysis

To validate the robustness of the primary findings, sensitivity analyses were conducted across multiple dimensions, including data completeness (complete-case analysis), unmeasured confounding (E-value), reverse causality (excluding deaths within 2 and 5 years), medication interference (excluding users of glucose-lowering or lipid-lowering agents), baseline diseases (excluding patients with pre-existing CVD, cancer, or CKD), additional adjustment for renal function, and competing risks (Fine–Gray model; see **Tables S5–S17**). Sensitivity analyses showed generally consistent results: the positive associations of TyG-ABSI with mortality in the overall population, MUNO, and MUO remained robust (HR range 1.14–1.32); MHNO showed only marginal significance; and no significant association was observed in MHO across all analyses. These findings suggest that the observed associations are not solely attributable to specific analytical approaches, although residual confounding and selection bias cannot be fully excluded.

After additional adjustment for the five MetS components (**Table S16**), the association in MUO was largely attenuated (all-cause: adjusted HR = 1.15, P = 0.155; CVD: adjusted HR = 1.05, P = 0.755), whereas MUNO retained significant associations (all-cause: HR = 1.27, P < 0.001; CVD: HR = 1.49, P = 0.001). This indicates that in MUO, the prognostic information conveyed by TyG-ABSI is largely captured by conventional MetS components, whereas in MUNO, TyG-ABSI provides independent prognostic value beyond MetS components.

In the Fine-Gray subdistribution hazard model treating non-CVD death as a competing risk, the association between TyG-ABSI and CVD mortality remained significant in the overall population (SHR = 1.21, 95% CI 1.10–1.32, *P* < 0.001; **Table S17**).

4 Discussion

This study provides the first phenotype-stratified evaluation of the prognostic value of TyG-ABSI for mortality across MetS-related metabolic health–obesity phenotypes. The key finding is that the independent prognostic value of TyG-ABSI was most consistent in MUNO, whereas in MUO the association was largely explained by conventional MetS components, and in MHO no statistically significant association was detected. In MHNO, a nonlinear dose–response relationship was observed, around a Z-score of approximately 2.1 (TyG-ABSI ≈ 0.86). In the MUO phenotype, an exploratory ePWV-related effect modification was observed for all-cause mortality in the primary stratified analysis (*P* for interaction = 0.022), but this signal was attenuated after adjustment for TyG-ABSI × age and TyG-ABSI × SBP. Because ePWV is estimated from age and SBP, this finding should not be equated with the biological effect of arterial stiffness itself. Exploratory analyses of systemic inflammatory markers (SIRI, SII, and AISI) showed minimal associations and should be interpreted as inconclusive.

4.1 An integrated interpretation of the phenotypic heterogeneity of TyG-ABSI

4.1.1 Pathophysiological basis of TyG-ABSI phenotypic heterogeneity

The association between TyG-ABSI and mortality differed across MetS-related metabolic phenotypes. In metabolically unhealthy phenotypes, insulin resistance, lipotoxicity, and oxidative stress may jointly contribute to multisystem injury [20-25]. In MHNO, the nonlinear pattern may reflect a transition from early metabolic compensation to decompensation at extremely high TyG-ABSI levels; however, this threshold was derived from a single NHANES analysis and was not replicated in CHARLS. It should therefore be regarded as hypothesis-generating and requires exploratory cross-population comparison before any clinical use. Because the exploratory association decomposition analysis in MHO was not statistically significant, phenotype-specific mechanisms for MHO were not further explored.

4.1.2 Dialogue with the controversial literature on MHO

The null finding in MHO should be interpreted in the context of the ongoing controversy surrounding this phenotype. Although some studies classify MHO as a "low-risk" state, substantial evidence suggests that it represents a "delayed risk," with cardiovascular risk remaining higher than in MHNO during long-term follow-up [26-29]. In the present study, TyG-ABSI showed no statistically significant association with mortality in MHO; however, this subgroup had limited events and wide confidence intervals, and the study was underpowered to detect modest associations. TyG-ABSI may not be the optimal standalone biomarker for risk stratification in MHO, rather than being definitively ineffective. Consistent with this, all TyG-derived indices showed limited discriminative performance in MHO, and no significant TyG-ABSI × ePWV interaction was observed. MHO-related risk may be less dependent on insulin resistance and may involve mechanical cardiac load, neuroendocrine dysregulation, sleep apnea, or other pathways not captured by TyG-ABSI. For clinical practice, TyG-ABSI should not be used as a standalone screening tool in MHO; risk assessment may require alternative or complementary markers, such as high-sensitivity C-reactive protein, carotid intima-media thickness, sleep apnea assessment, or body composition measures.

4.1.3 Comparison with existing evidence on TyG-ABSI

The effect estimates from the primary analysis in the general population (all-cause: HR = 1.19 per SD; cardiovascular: HR = 1.27 per SD) were largely consistent with previous findings. He et al. [12] reported an HR of 1.29 for cardiovascular mortality, Yang et al. [13] reported an HR of 1.21 for all-cause mortality in MASLD, and Su et al. [14] obtained similar results in hypertensive populations. However, these studies did not examine whether the association is modified by metabolic health–obesity phenotype. The present study extends this evidence by demonstrating that the independent prognostic value of TyG-

ABSI is phenotype-dependent: it is retained in MUNO but largely explained by conventional MetS components in MUO, and not statistically significant in MHO.

This distinction has direct clinical implications—rather than applying TyG-ABSI uniformly, its use should be prioritized in MUNO (where conventional criteria may miss occult visceral adiposity and insulin resistance) and de-emphasized in MUO (where standard MetS components already capture the prognostic information). After additional adjustment for the five MetS components (**Table S16**), the association was largely explained in MUO (adjusted HR = 1.15, $P = 0.155$), whereas it remained independent in MUNO (Q4 vs. Q1: all-cause HR = 1.65, $P < 0.001$; cardiovascular HR = 1.94, $P < 0.001$). This may be clinically relevant because individuals with normal waist circumference are often overlooked in routine assessment, and an elevated TyG-ABSI in such individuals may signal occult visceral adiposity and insulin resistance, warranting more comprehensive cardiovascular risk evaluation.

4.2 Potential Mechanisms

4.2.1 ePWV-Related Vascular Aging as a Preliminary Effect Modifier and Potential Additional Pathways

In the primary stratified analysis, an exploratory ePWV-related effect modification was observed in MUO, but this signal was attenuated after additional adjustment for TyG-ABSI × age and TyG-ABSI × SBP. Because ePWV is estimated from age and SBP rather than directly measured, this finding should be regarded as exploratory evidence for an ePWV-related vascular aging process, not as proof of an independent biological effect of arterial stiffness. The attenuation is consistent with the broader observation that MUO-related prognostic information conveyed by TyG-ABSI is largely captured by conventional MetS components and age/SBP. Future studies using directly measured cfPWV are needed.

For all-cause mortality, the association was significant in the highest ePWV tertile, but no significant interaction was observed in MHNO or MUNO; patterns were similar for cardiovascular mortality, with

no effect modification in MHO.

Several additional pathways may contribute to the association between TyG-ABSI and mortality, including hyperglycemia-induced endothelial dysfunction [30], oxidized LDL accumulation and foam cell formation [31, 32], insulin resistance–related increases in PAI-1 and thrombotic risk [33, 34], and cardiac autonomic neuropathy [30]. These possibilities are speculative and require further investigation.

4.2.2 A cautious interpretation of the preliminary association decomposition in the MHO group

In the MHO phenotype, no statistically significant TyG-ABSI × ePWV interaction was observed for either outcome. This is consistent with the overall null finding in MHO, but given the limited number of events, it should not be interpreted as evidence of no association.

4.2.3 The limited role of inflammatory markers

In exploratory analyses, systemic inflammatory markers (SIRI, SII, and AISI) showed minimal associations with the TyG-ABSI–mortality association (explained proportions ≤ 7%). These findings suggest that systemic inflammation is unlikely to be a major pathway linking TyG-ABSI to mortality, although these analyses were exploratory and measured at the same baseline time point as the exposure.

4.2.4 Biological explanations for subgroup differences

Among subgroup findings, the age interaction was the most consistent, with a stronger association in younger participants, possibly reflecting greater reversibility of metabolic risk at earlier stages. The sex interaction was also notable but should be interpreted cautiously given multiple testing. Other subgroup interactions, including cancer history and metabolic risk factors, were exploratory and require confirmation in independent cohorts.

4.3 Clinical Significance

4.3.1 Stratified application recommendations

In MHO, all TyG-derived indices showed limited discriminative performance, and TyG-ABSI

showed no significant association across ePWV strata. Based on current evidence, TyG-ABSI is not recommended as a standalone screening tool in MHO; risk assessment may require alternative biomarkers such as high-sensitivity C-reactive protein, carotid intima-media thickness, or sleep apnea assessment. Given the limited number of events, this recommendation should be interpreted with caution. The hypothesis-generating Z-score threshold around 2.1 in MHNO requires cross-population comparison and is not currently recommended for clinical decision-making.

4.3.2 Connection to specific interventions

For individuals with metabolic dysfunction and elevated TyG-ABSI, lifestyle intervention and comprehensive metabolic risk management remain the foundation. Pharmacological therapies such as GLP-1 receptor agonists and SGLT2 inhibitors may have additional metabolic and cardiovascular benefits [35-40], and statins may reduce cardiovascular risk in selected populations [41, 42]. However, the specific role of TyG-ABSI in guiding these interventions requires further study.

4.4 Advantages and Limitations

Advantages: This study used a large, representative cohort (NHANES, N = 20,430) with a median follow-up of 115 months, applying multiple imputation and complex sampling weights. Analyses included Cox proportional hazards models, RCS, Fine–Gray competing risk models, NRI/IDI, DCA, and 13 sensitivity analyses, complemented by Boruta feature selection, VIF-based collinearity exclusion, and the EPV principle. Phenotype stratification was prespecified rather than post hoc.

Limitations: First, the observational design precludes causal inference, although E-values suggested moderate robustness to unmeasured confounding. Second, external generalizability is constrained: the primary NHANES findings were not replicated in CHARLS, which may reflect racial differences, heterogeneity in diagnostic criteria, dietary patterns, absence of cause-specific mortality data, and shorter

follow-up. Obesity was defined as BMI ≥ 30 kg/m² in NHANES but ≥ 28 kg/m² in CHARLS, and MetS criteria differed between AHA/NHLBI and Chinese guidelines. The CHARLS analysis should therefore be considered exploratory, and the non-replication underscores the need for further validation rather than excluding a possible association in other populations. Third, the analytic cohort was derived after multiple exclusions, and excluded participants were not systematically compared with the analytic cohort; selection bias cannot be fully excluded. Fourth, CVD and cancer history were based on self-reported physician diagnosis, which may be subject to recall bias and misclassification, an inherent limitation of NHANES-based research. Fifth, baseline measurements may be subject to single-measurement bias and cannot capture dynamic changes in metabolic status during follow-up (e.g., MHO-to-MUO transition, weight fluctuations, medication adjustments). Sixth, the MHO group had a relatively small sample size (n = 2,920), resulting in limited statistical power; because no events occurred in the MHO group in CHARLS, this phenotype was excluded from that analysis, and the null findings should be interpreted with caution (type II error cannot be excluded). Seventh, the exploratory association decomposition analysis (**Table S20**) was based on baseline data, with ePWV and TyG-ABSI measured at the same time point; it should be regarded as exploratory evidence of association rather than a basis for causal inference. Eighth, because TyG-ABSI is a composite index, the independent contributions of its components require further decomposition; future studies could use causal mediation analysis or structural equation modeling to quantify their relative weights.

5 Conclusion

Across MetS-related metabolic health–obesity phenotypes, TyG-ABSI showed phenotype-depend-

ent prognostic performance, with the most consistent independent value in MUNO. In MUO, its association was largely explained by conventional MetS components. In MHO, no statistically significant association was detected, but this should not be interpreted as proof of no effect, and larger studies are required. An ePWV-related vascular aging process modified the TyG-ABSI–all-cause mortality association in MUO in the primary stratified analysis (*P* for interaction = 0.022), but this preliminary finding was attenuated after adjustment for age and SBP interactions and should not be equated with the biological effect of arterial stiffness itself. These findings were derived from a U.S. nationwide cohort; their generalizability to Asian populations remains uncertain, and the non-replication in CHARLS highlights the need for further external validation across diverse populations.

Abbreviations

ABSI: A Body Shape Index

AISI: Age-adjusted Systemic Inflammation Index

ALT: Alanine Aminotransferase

Anti-DM meds: Anti-diabetic medications

Anti-Hypertension meds: Anti-hypertensive medications

AST: Aspartate Aminotransferase

AUC: Area Under the Curve

BMI: Body Mass Index

BRI: Body Roundness Index

CHARLS: China Health and Retirement Longitudinal Study

CI: Confidence Interval

589 CKD: Chronic Kidney Disease

590 CVD: Cardiovascular Disease

591 DBP: Diastolic Blood Pressure

592 DCA: Decision Curve Analysis

593 DM: Diabetes Mellitus

594 ePWV: Estimated Pulse Wave Velocity

595 HDL-C: High-Density Lipoprotein Cholesterol

596 HR: Hazard Ratio

597 IDI: Integrated Discrimination Improvement

598 LAP: Lipid Accumulation Product

599 LDL-C: Low-Density Lipoprotein Cholesterol

600 Lipid-lowering meds: Lipid-lowering medications

601 MET: Metabolic Equivalent of Task

602 MetS: Metabolic Syndrome

603 MHNO: Metabolically Healthy Non-Obesity

604 MHO: Metabolically Healthy Obesity

605 MUNO: Metabolically Unhealthy Non-Obesity

606 MUO: Metabolically Unhealthy Obesity

607 NHANES: National Health and Nutrition Examination Survey

608 NRI: Net Reclassification Improvement

609 PIR: Poverty Income Ratio

610 RCS: Restricted Cubic Spline

ROC: Receiver Operating Characteristic

SBP: Systolic Blood Pressure

SD: Standard Deviation

SII: Systemic Immune-Inflammation Index

SIRI: Systemic Inflammation Response Index

TyG: Triglyceride-Glucose Index

TyG-ABSI: Triglyceride-Glucose-Body Shape Index

TyG-BMI: Triglyceride-Glucose-Body Mass Index

TyG-BRI: Triglyceride-Glucose-Body Roundness Index

TyG-LAP: Triglyceride-Glucose-Lipid Accumulation Product

TyG-VAI: Triglyceride-Glucose-Visceral Adiposity Index

TyG-WC: Triglyceride-Glucose-Waist Circumference

TyG-WHtR: Triglyceride-Glucose-Waist-to-Height Ratio

TyG-WWI: Triglyceride-Glucose-Weight-adjusted Waist Index

VAI: Visceral Adiposity Index

WC: Waist Circumference

WHtR: Waist-to-Height Ratio

WWI: Weight-adjusted Waist Index

Declarations

Informed consent

The NHANES study protocol received approval from the Institutional Review Board of the National Center for Health Statistics, and all participants provided written informed consent prior to enrollment.

Ethics approval and consent to participate

The NHANES protocol was approved by the NCHS Research Ethics Review Board (ERB), and all participants provided written informed consent. The CHARLS study was approved by the Peking University Institutional Review Board (IRB00001052-11015), with written informed consent obtained from all participants. As this was a secondary analysis of de-identified, publicly available data conducted in accordance with the Declaration of Helsinki, additional ethical approval was not required.

Consent for publication

Not applicable.

Trial registration

Clinical trial number: not applicable.

Data availability

The NHANES and CHARLS datasets analyzed in this study are publicly accessible at https://www.cdc.gov/nchs/nhanes/ and http://charls.pku.edu.cn, respectively, subject to registration or data use agreements.

Competing interests

The authors declare that they have no competing interests.

Funding

This research received no specific grant from any funding agency in the public, commercial, or not-for-profit sectors.

Authors' contributions

Q.X. and M.L. conceived and designed the study. M.X. and Q.X. acquired and analysed the data. Q.X., M.X., and M.L. interpreted the results. Q.X. drafted the manuscript. M.L. contributed to manuscript refinement, provided expert input, supervised the research process, and ensured quality control. All authors critically revised the manuscript for important intellectual content and approved the final version for submission.

Acknowledgements

The authors thank the National Center for Health Statistics (NCHS) for the NHANES data and the CHARLS research team at Peking University for the CHARLS data. We also thank all study participants and fieldworkers for their contributions.

References

1. Collaborators GRF. Burden of 375 diseases and injuries, risk-attributable burden of 88 risk factors, and healthy life expectancy in 204 countries and territories, including 660 subnational locations, 1990-2023: a systematic analysis for the Global Burden of Disease Study 2023. Lancet. 2025;406(10513):1873-922.
2. Collaborators GDaI. Global incidence, prevalence, years lived with disability (YLDs), disability-adjusted life-years (DALYs), and healthy life expectancy (HALE) for 371 diseases and injuries in 204 countries and territories and 811 subnational locations, 1990-2021: a systematic analysis for the Global Burden of Disease Study 2021. Lancet. 2024;403(10440):2133-61.
3. Valenzuela PL, Carrera-Bastos P, Castillo-García A, Lieberman DE, Santos-Lozano A, Lucia A. Obesity and the risk of cardiometabolic diseases. Nat Rev Cardiol. 2023;20(7):475-94.
4. Schulze MB, Stefan N. Metabolically healthy obesity: from epidemiology and mechanisms to clinical implications. Nat Rev Endocrinol. 2024;20(11):633-46.
5. Son DH, Ha HS, Park HM, Kim HY, Lee YJ. New markers in metabolic syndrome. Adv Clin Chem. 2022;110:37-71.
6. Islam MS, Wei P, Suzauddula M, Nime I, Feroz F, Acharjee M, et al. The interplay of factors in metabolic syndrome: understanding its roots and complexity. Mol Med. 2024;30(1):279.
7. Tian X, Chen S, Wang P, Xu Q, Zhang Y, Luo Y, et al. Insulin resistance mediates obesity-related risk of cardiovascular disease: a prospective cohort study. Cardiovasc Diabetol. 2022;21(1):289.
8. Sawaf B, Swed S, Alibrahim H, Bohsas H, Dave T, Nasif MN, et al. Triglyceride-Glucose Index as Predictor for Hypertension, CHD and STROKE Risk among Non-Diabetic Patients: A NHANES Cross-Sectional Study 2001-2020. J Epidemiol Glob Health. 2024;14(3):1152-66.
9. Luengo-Fernandez R, Walli-Attaei M, Gray A, Torbica A, Maggioni AP, Huculeci R, et al. Economic burden of cardiovascular diseases in the European Union: a population-based cost study. Eur Heart J. 2023;44(45):4752-67.
10. Liu X, Yang S, Fu Q, Sun Y, Jing S, Liu M, et al. Predictive value of the triglyceride glucose index-a body shape index (TyG-ABSI) for cardiovascular disease and its comparison with other TyG-related obesity indices: a study based on the China health and retirement longitudinal study (CHARLS) cohort. Cardiovasc Diabetol. 2026;25(1):227.
11. Lu CY, Chen HH, Chi KH, Chen PC. Obesity indices and the risk of total and cardiovascular mortality among people with diabetes: a long-term follow-up study in Taiwan. Cardiovasc Diabetol. 2023;22(1):345.
12. He HM, Xie YY, Chen Q, Li YK, Li XX, Fu SJ, et al. The synergistic effect of the triglyceride-glucose index and a body shape index on cardiovascular mortality: the construction of a novel cardiovascular risk marker. Cardiovasc Diabetol. 2025;24(1):69.
13. Yang G, He W, Qiu X, Shen S, Li P, Feng Y, et al. Triglyceride glucose index-a body shape index (TyG-ABSI) outperforms traditional obesity indices in predicting all-cause

and cardiovascular mortality in metabolic-dysfunction associated steatotic liver disease: the mediating role of biological aging. Cardiovasc Diabetol. 2026;25(1):102.
14. Su Q, Qin Y, Huang WZ, Mo LR, Yang HF, Wu Q. First Comparative Evaluation of TyG-ABSI Versus Traditional TyG-Related Indices for Cardiovascular Disease and Mortality Prediction in Hypertensive Patients: TyG-ABSI Versus Traditional TyG-Related Indices. J Clin Hypertens (Greenwich). 2026;28(6):e70301.
15. Zheng X, Zhang W, Yang F, Wang L, Yu B, Liang B. Evaluative performance of TyG-ABSI versus traditional indices in relation to cardiovascular disease and mortality: evidence from the U.S. NHANES. Cardiovasc Diabetol. 2025;24(1):344.
16. Alberti KG, Eckel RH, Grundy SM, Zimmet PZ, Cleeman JI, Donato KA, et al. Harmonizing the metabolic syndrome: a joint interim statement of the International Diabetes Federation Task Force on Epidemiology and Prevention; National Heart, Lung, and Blood Institute; American Heart Association; World Heart Federation; International Atherosclerosis Society; and International Association for the Study of Obesity. Circulation. 2009;120(16):1640-5.
17. Guerrero-Romero F, Simental-Mendía LE, González-Ortiz M, Martínez-Abundis E, Ramos-Zavala MG, Hernández-González SO, et al. The product of triglycerides and glucose, a simple measure of insulin sensitivity. Comparison with the euglycemic-hyperinsulinemic clamp. J Clin Endocrinol Metab. 2010;95(7):3347-51.
18. VanderWeele TJ. Causal mediation analysis with survival data. Epidemiology. 2011;22(4):582-5.
19. VanderWeele TJ, Ding P. Sensitivity Analysis in Observational Research: Introducing the E-Value. Ann Intern Med. 2017;167(4):268-74.
20. Saadati S, Godini R, Reddy A, Teede H, Mousa A. Metabolic crossroads in insulin resistance: exploring lipid dysregulation and inflammation. Front Immunol. 2025;16:1692742.
21. Bansal SK, Bansal MB. Pathogenesis of MASLD and MASH - role of insulin resistance and lipotoxicity. Aliment Pharmacol Ther. 2024;59 Suppl 1:S10-s22.
22. Bordoni L, Mansouri F, Rucci C, Agostinho de Sousa J, von Meyenn F. Associations between dietary food categories, epigenetic age acceleration and low-grade inflammation in the Lifelines-DEEP cohort. Clin Nutr. 2026;63:106703.
23. Fasciolo G, Napolitano G, Aprile M, Cataldi S, Costa V, Muscari Tomajoli MT, et al. Muscle Oxidative Stress Plays a Role in Hyperthyroidism-Linked Insulin Resistance. Antioxidants (Basel). 2023;12(3).
24. Guo Y, Ma Q, Guo Z, Chu J, Wu N, Qi Y. Inflammation-mediated diabetes-liver disease cross-organ crosstalk: From molecular mechanisms to precision therapeutic strategies. Life Sci. 2026;402:124534.
25. Fallah F, Mahdavi R. L-Carnitine and synbiotic co-supplementation: beneficial effects on metabolic-endotoxemia, meta-inflammation, and oxidative-stress biomarkers in obese patients: a double blind, randomized, controlled clinical trial. Food Funct. 2023;14(4):2172-87.
26. Copur S, Tanriover C, Yavuz F, Tuttle KR, Kanbay M. Tirzepatide and potential use for metabolically healthy obesity. Eur J Intern Med. 2023;113:1-5.

27. Gao JW, You S, Liu ZY, Hao QY, Wang JF, Vuitton DA, et al. Different Metabolic Phenotypes of Obesity and Risk of Coronary Artery Calcium Progression and Incident Cardiovascular Disease Events: The CARDIA Study. Arterioscler Thromb Vasc Biol. 2022;42(5):677-88.
28. Putri RR, Danielsson P, Hagman E, Marcus C. Long-Term Cardiometabolic Outcomes in Children With Metabolically Healthy and Unhealthy Obesity. JAMA Pediatr. 2026;180(7):750-7.
29. Blaak EE, Goossens GH. Metabolic phenotyping in people living with obesity: Implications for dietary prevention. Rev Endocr Metab Disord. 2023;24(5):825-38.
30. Caturano A, Rocco M, Tagliaferri G, Piacevole A, Nilo D, Di Lorenzo G, et al. Oxidative Stress and Cardiovascular Complications in Type 2 Diabetes: From Pathophysiology to Lifestyle Modifications. Antioxidants (Basel). 2025;14(1).
31. Wang Z, Chen J, Zeng Z, Zhang Q, Du G, Guo X, et al. The LOX-1 receptor ectopically expressed in the liver alleviates atherosclerosis by clearing Ox-LDL from the circulation. Mol Med. 2022;28(1):26.
32. Wang H, Guo J, Xiu T, Tang Y, Li P, Zhang W, et al. H(2)O(2) accumulation promoting internalization of ox-LDL in early atherosclerosis revealed via a synergistic dual-functional NIR fluorescence probe. Chem Sci. 2024;16(1):345-53.
33. Ferraresso F, Skaer CW, Wei Z, Hur WS, Yu H, Seadler M, et al. Silencing of PAI-1 using siRNA-lipid nanoparticles reduces thrombosis and prolongs life span in murine models. Blood. 2026;147(18):2053-63.
34. Kocabas S, Sanlier N. Plasminogen activator inhibitor-1, vaspin, and dietary inflammatory index in relation to cardiometabolic health in diabetic women. Front Nutr. 2026;13:1784603.
35. Tschop M, Nogueiras R, Ahren B. Gut hormone-based pharmacology: novel formulations and future possibilities for metabolic disease therapy. Diabetologia. 2023;66(10):1796-808.
36. Rosen CJ, Ingelfinger JR. GLP-1 Receptor Agonists. N Engl J Med. 2026;394(13):1313-24.
37. Mashayekhi M, Nian H, Mayfield D, Devin JK, Gamboa JL, Yu C, et al. Weight Loss-Independent Effect of Liraglutide on Insulin Sensitivity in Individuals With Obesity and Prediabetes. Diabetes. 2024;73(1):38-50.
38. Soares RN, Ramirez-Perez FI, Cabral-Amador FJ, Morales-Quinones M, Foote CA, Ghiarone T, et al. SGLT2 inhibition attenuates arterial dysfunction and decreases vascular F-actin content and expression of proteins associated with oxidative stress in aged mice. Geroscience. 2022;44(3):1657-75.
39. Liu L, Ni YQ, Zhan JK, Liu YS. The Role of SGLT2 Inhibitors in Vascular Aging. Aging Dis. 2021;12(5):1323-36.
40. Armillotta M, Angeli F, Paolisso P, Belmonte M, Raschi E, Di Dalmazi G, et al. Cardiovascular therapeutic targets of sodium-glucose co-transporter 2 (SGLT2) inhibitors beyond heart failure. Pharmacol Ther. 2025;270:108861.
41. Yoo J, Jeon J, Baek M, Song SO, Kim J. Impact of statin treatment on cardiovascular risk in patients with type 1 diabetes: a population-based cohort study. J Transl Med.

2023;21(1):806.
42. Wang L, Zheng Z, Zhu L, Meng L, Liu H, Wang K, et al. Geranylgeranyl pyrophosphate depletion by statins compromises skeletal muscle insulin sensitivity. J Cachexia Sarcopenia Muscle. 2022;13(6):2697-711.

Supplementary Files

This is a list of supplementary files associated with this preprint. Click to download.

- SupplementaryMaterial1.docx
- SupplementaryMaterial2.docx
- Supplementarymaterial3.docx
- Supplementarymaterial4.docx
- Supplementarymaterial5STROBEchecklistv4cohort.doc